# Effective use of cerium anomalies as a redox proxy in carbonate-dominated marine settings

Rosalie Tostevin [a],*, Graham A. Shields [a], Gary M. Tarbuck [a], Tianchen He [a], Matthew O. Clarkson [b], Rachel A. Wood [c]

[a] University College London, Department of Earth Sciences, Gower Street, London WC1E 6BT, UK
[b] University of Otago, Department of Chemistry, Union Place West, Dunedin 9016, New Zealand
[c] The University of Edinburgh, School of GeoSciences, James Hutton Road, Edinburgh EH9 3FE, UK

## ABSTRACT

Rare earth elements and yttrium (REY) have a distinct distribution pattern in seawater, and this pattern may be faithfully preserved in carbonate sediments and rocks. Anomalous concentrations of redox-sensitive cerium (Ce) compared with neighbouring REY originate in oxic water column conditions, and as such, Ce anomalies can provide a potentially useful redox proxy in carbonate-dominated marine settings. The methods used to extract REY from carbonates vary widely, and may suffer from widespread leaching of REY from accessory non-carbonate minerals and organic matter, limiting the application of Ce anomalies for palaeo-redox reconstruction. We have systematically compared different methods on 195 carbonate samples with varying purity (% carbonate) from both modern and ancient environments. We used sequential leaching experiments in nitric acid to identify the most 'seawater-like' portion of the carbonate sample where contributions from non-carbonate minerals and organic matter are minimised. We also compared the results of sample dissolution in different types and strengths of acid. Our results confirm that REY concentrations can be inadvertently contaminated by partial leaching of clays and Fe (oxyhydr)oxides during a single-step digestion, and we suggest a pre-leach of 20% of the sample, followed by a partial leach of 40% of the sample to selectively dissolve carbonate. We suggest that REY studies are optimised in carbonates with >85% CaCO$_3$, and show that dolomites behave differently during the leaching process and must be treated separately. We present REY patterns for modern carbonate-rich sediments from a range of environments, and show that seawater REY are faithfully preserved in some non-skeletal carbonate, but modified leaching procedures are necessary for impure, unlithified or organic rich carbonate sediments. We combine REY with Fe-speciation data to identify how Fe oxides and clays contribute to the REY signal and explore how the two proxies can be used together to provide a complex and high-resolution redox reconstruction in carbonate-dominated marine environments.

## 1. Introduction

### 1.1. The rare earth elements in seawater

The lanthanides, or rare earth elements (REE), consist of fourteen elements that form a series from the lightest (lanthanum, La) to the heaviest (lutetium, Lu). Yttrium (Y) is often included alongside the lanthanides as it has similar chemical properties to Holmium (Ho). Rare earth elements and yttrium (REY) are supplied to the ocean through rivers, Aeolian input and hydrothermal vents, and are removed during sedimentation via particle scavenging (Byrne and Kim, 1990; Douville et al., 1999; Elderfield et al., 1990). Their exceptionally similar chemical properties mean they behave coherently, resulting in smooth, predictable distribution patterns when normalized to PAAS (post Archean Australian Shale, Pourmand et al., 2012). Normalisation is a common practice as it removes the natural variations in absolute concentrations of REY and allows a comparison with the REY composition of the upper crust, for which shale is a proxy. Hydrothermal input represents a large, but likely secondary flux of REY to the ocean, and carries a flat or heavy rare earth (HREE) depleted REY signal with excess europium (Eu) concentrations (Fig. 1) (Bau and Dulski, 1996; Douville et al., 1999). Rivers are a major source of REY, and carry a flat 'continental type' shale-normalized distribution pattern, but when freshwater interacts with saline waters in estuaries, REY rapidly acquire a typical 'seawater type' pattern with characteristic anomalies (Fig. 1) (Elderfield et al., 1990).

The typical seawater REY profile (Fig. 1) is smooth and coherent with progressive enrichments in heavier REE. REE(III) mono– and di–carbonate ion complexes are the dominant dissolved species in seawater, and the filling of the 4f electron shell across the series results in a systematic increase in

* Corresponding author at: Department of Earth Science, University of Oxford, South Parks Road, OX13AN, UK.
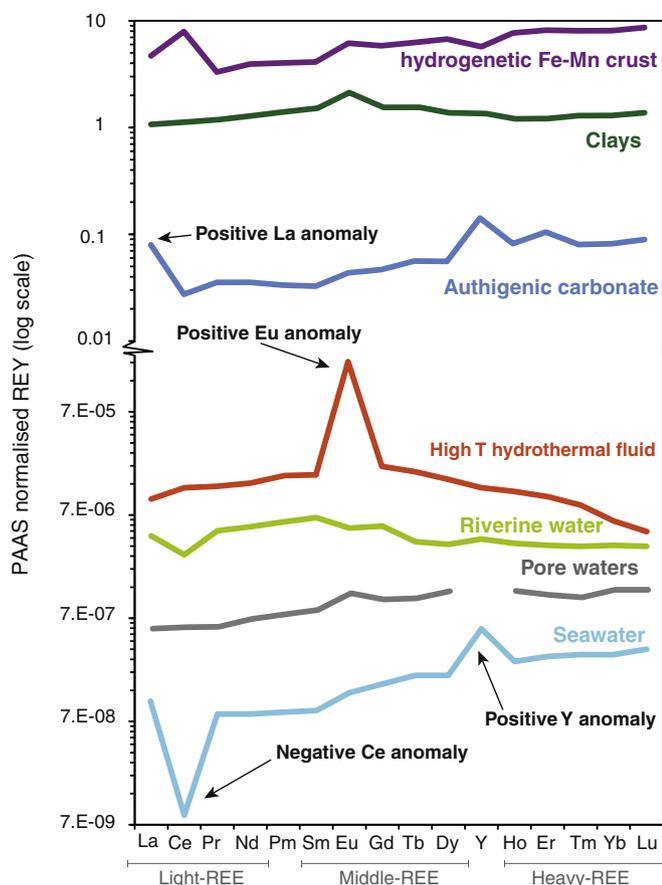  *E-mail address:* Rosalie.tostevin@earth.ox.ac.uk (R. Tostevin).

**Fig. 1.** Shale normalized REY patterns representing key natural environments and minerals, showing typical anomalous features such as Ce, La, Eu and Y anomalies. While some of these distribution patterns are near universal (e.g. seawater), others will vary significantly on a local scale (e.g. pore waters). The rare earth elements are grouped into light (LREE), medium (MREE) and heavy (HREE). Data are based on reported REY, with marine hydrogenetic Fe-Mn crusts and high-temperature hydrothermal (black-smoker) fluids from Bau and Dulski (1996), modern seawater from James et al. (1995), marine pore water from Haley et al. (2004), riverine water from Soyol-Erdene and Huh (2013), and authigenic carbonate and clays from Zebra River (this study).

carbonate complexation from the light to the heavier REE (Byrne and Kim, 1990; Zhong and Mucci, 1995). This leaves seawater enriched in heavier REE, and the enrichment ratio is often quantified using the shale normalized ytterbium/neodymium ($Yb_{SN}/Nd_{SN}$) ratio. Deviations from this smooth slope occur where an element in the series has a unique chemical property that affects its solubility and removal via scavenging onto Fe-Mn (oxyhydr)oxides, organic matter and clay particles. In modern seawater this results in positive Y, La, Eu, gadolinium (Gd) and Lu anomalies, and negative Ce anomalies.

Modern seawater contains a large positive Y anomaly (mass ratio of Y to Ho), with larger Y anomalies (40–80) occurring in open marine settings and smaller Y anomalies (33–40) in near shore or restricted settings (Bau et al., 1997; De Baar et al., 1985a, 1985b; Nozaki and Zhang, 1995). Y/Ho also varies with salinity, phosphate mineral solubility, and fractionation during chemical weathering, biological processes and redox cycling (Hill et al., 2000; Liu and Byrne, 1997). Our understanding of Y anomalies is somewhat limited, as many earlier studies did not include Y measurements alongside REEs (e.g. De Baar et al., 1985a). Small relative enrichments in La, Gd and Lu are possibly a consequence of their respective empty, half-filled and full 4f electron shells, which increase their relative stability in solution (Byrne and Kim, 1990; Byrne et al., 1996; De Baar et al., 1985b; Bolhar et al., 2004). Gd anomalies are generally small, and where great, may be an analytical artifact due to interferences with other ions of similar mass/charge ratio. The presence of these anomalies, particularly Y/Ho >36, is often used to support the preservation of unaltered seawater REY patterns in the marine rock record.

REY are typically in the +3 oxidation state, but Eu can occur in the +2 oxidation state in strongly reducing environments. Seawater shows variable but small positive Eu anomalies (around 1.5). Eu anomalies can be calculated by comparison with neighbouring REE:

$$Eu_{SN}/Eu_{SN}^* = \frac{2 * [Eu]_{S\,N}}{[Sm]_{SN} + [Gd]_{SN}} \tag{1}$$

Larger positive Eu anomalies may be present where seawater has mixed with hydrothermal fluids (Meyer et al., 2012). Apparent Eu anomalies may result from interference with barium oxides formed during analysis, and this can be evaluated through measurement of Ba concentrations (Jarvis et al., 1989).

REY patterns may also contain redox sensitive Ce anomalies (Bodin et al., 2013; Meyer et al., 2012; Schroder and Grotzinger, 2007). Ce is unique among the REY because it can exist in both the +3 and +4 oxidation state. In the presence of oxygen, Ce(III) is partially oxidised to Ce(IV) on the surface of Mn (oxyhydr)oxides, where it no longer participates in solid-solution exchange reactions, leaving residual seawater depleted in Ce relative to other trivalent REE (German and Elderfield, 1990). This fractionation of Ce only occurs under oxic conditions (German et al., 1991). Ce anomalies ($Ce_{SN}/Ce_{SN}^*$) are traditionally calculated by comparing the normalized concentration of Ce ($[Ce]_{SN}$) with its neighbouring REE:

$$Ce_{SN}/Ce_{SN}^* = \frac{2 * [Ce]_{SN}}{[La]_{SN} + [Pr]_{SN}} \tag{2}$$

The anomalous behaviour of La can artificially exaggerate the Ce anomaly. A more appropriate way to calculate Ce anomalies, avoiding comparison with La, was proposed by Lawrence et al. (2006), and has been used throughout this study:

$$Ce_{SN}/Ce_{SN}^* = \frac{[Ce]_{SN}}{([Pr]_{SN})^2/[Nd]_{SN}} \tag{3}$$

Negative Ce anomalies are ubiquitous in the modern, well-oxygenated ocean, but their magnitude varies within and between ocean basins (De Baar et al. 1985a, De Baar, 1991), and can respond to changes in water column redox on a meter scale (e.g De Carlo and Green, 2002). The relative importance of Fe and Mn (oxyhydr)oxides in the oxidation and scavenging of Ce is debated (see Bau et al., 2014), but Mn is generally considered to be the main carrier phase for excess Ce (Edmonds and German, 2004; De Baar et al., 1988; De Carlo and Green, 2002; Sholkovitz et al., 1994; De Carlo, 2000; Bau, 1999; Ohta and Kawabe, 2001). Since both Ce and Mn have a high reduction potential, the formation of Ce-enriched Mn oxides requires elevated oxygen concentrations compared with oxic signals from redox proxies based on Fe-C-S and trace element systematics. In modern stratified water columns, negative Ce anomalies develop in the oxic surface waters and are eroded in intermediate conditions, with Ce anomalies absent in deeper fully anoxic waters (German et al., 1991). In some modern manganous waters, local positive Ce anomalies develop beneath the Mn (IV/II) redoxcline (Bau et al., 1997; De Baar et al., 1988; De Carlo and Green, 2002). These positive Ce anomalies have also been documented in carbonates from the late Ediacaran (Mazumdar et al., 2003) and Fe formations and cherts from the Palaeoproterozoic (Planavsky et al., 2010; Slack et al., 2007). Ce anomaly formation may be disrupted under strongly alkaline conditions (Möller and Bau, 1993; Pourret et al., 2008), in the presence of siderophores (Kraemer et al., 2015), as well as in surface waters due to photo-reduction of Mn oxides (Sunda and Huntsman, 1988).

The preservation of characteristic seawater anomalies in the REY distribution pattern in authigenic minerals can verify that the sample was deposited in open marine conditions and has not been secondarily altered, increasing confidence in other geochemical data and chemostratigraphy (Bolhar and Van Kranendonk, 2007; Frimmel, 2010). REY can also yield information about relative water depth and proximity to hydrothermal vents. These indicators must be interpreted with caution,

however, as wind borne dust can lend a terrestrial signature to coastal seawater, and some of the processes that act to fractionate REY in the ocean also operate in terrestrial waters, although to a lesser extent (Johannesson et al., 2006). The redox sensitive behaviour of Ce has been used to estimate the residence times of suspended particles in the upper ocean (Sholkovitz et al., 1994). Most commonly, Ce anomalies are used as a redox proxy to identify oxygenation of the marine environment during the Precambrian, or Phanerozoic anoxic events (Bodin et al., 2013; German and Elderfield, 1990; Kakuwa and Matsumoto, 2006; Ling et al., 2011; Liu et al., 1988; Riding et al., 2014; Schroder and Grotzinger, 2007).

### 1.2. Extracting seawater REY from rocks and sediments

Efforts to find a reliable proxy for seawater REY have included skeletal carbonate, apatites, and hydrogenous materials (e.g. marine chert, carbonate and phosphorite). REY substitute for the calcium ion in the calcite lattice, and can remain stable during diagenesis, including burial dolomitization and even dissolution–reprecipitation in some meteoric environments (Banner et al., 1988; Webb et al., 2009; Webb and Kamber, 2000). Although alteration of REY patterns during late stage diagenesis cannot be excluded, it can be identified via examination of the REY pattern and comparison with major and trace element data (Chen et al., 2015; Himmler et al., 2013, 2010). Here, we focus on marine carbonates formed at or close to the seafloor from the dissolved inorganic carbon pool, with the aim of reconstructing seawater REY patterns and associated redox sensitive Ce anomalies. Some studies target diagenetic carbonates, which here we consider 'contaminants', but the protocols we outline could potentially be adapted towards such work (Himmler et al., 2010).

Microbial and other non-skeletal carbonate may provide a more reliable proxy for seawater REY concentrations than skeletal carbonate (Webb and Kamber, 2000). This is because they incorporate REY concentrations ten times higher than skeletal carbonate and they usually directly precipitate carbonate without the use of complex mineralization pathways that may cause fractionation. Further, most non-skeletal carbonate is free from associated ferromanganese crusts. The preservation of REY in non-skeletal carbonate enables this proxy to be utilised in rocks >550 Ma, before the advent of abundant biologically controlled mineralization (Wood, 2011), and in both oxic and anoxic settings (Castanier, 1999). Microbialites can form in lacustrine, shallow and deep marine environments, but their formation may be influenced by a variety of prokaryotes (oxygenic and anoxygenic phototrophs, iron- and sulfate- reducing bacteria, methanogenic archaea), and our understanding of the uptake mechanisms of REY in microbialites and different inorganic carbonate phases is poor. Recent work suggests there may be some vital effects that result in fractionation (Johannesson et al., 2014).

A redox proxy that is effective in marine carbonate settings would be particularly powerful, as carbonates account for a large proportion of the rock record and often represent ecologically important reef and other biodiverse tropical and non-tropical shelf environments, and can provide complementary information such as strontium isotopes, carbon isotopes, and sulfur isotopes of seawater sulfate. Iodine/calcium ratios have been effectively applied to carbonate rocks (Lu et al., 2010), but many other local redox proxies remain untested. Clarkson et al. (2014) recently calibrated Fe-speciation in carbonate settings, but this proxy is only applicable in samples with >0.5 wt% $Fe_T$. The tendency towards low $Fe_T$ in oxygenated conditions, particularly in shallow water settings, can limit the application of Fe speciation in carbonates, but Ce anomalies do not suffer from these constraints.

If seawater REY patterns are faithfully preserved in authigenic carbonate sediments and rocks, it is necessary to ensure the signal can be effectively extracted during the leaching process, as the leaching of non-carbonate phases with high concentrations of REY can overwhelm the signal from the authigenic inventory. Any mixing with non-carbonate phases usually results in increased LREEs and weakening of any Ce anomaly, together with a decrease in the Y/Ho ratio and the development of a small Eu anomaly (Fig. 1). The most likely type of contaminant is fine-grained clastics such

as quartz-feldspars and clay minerals, which would have a flat REY pattern, lacking many of the anomalies characteristic of marine deposits (Fig. 1; Pourmand et al., 2012). Diagenetic phosphates can form during lithification and their REY signal often exhibits middle-REE enrichments (Haley et al., 2004; Martin et al., 2010; McArthur and Walsh, 1984). A high bell-shaped index can be used to approximate post depositional enrichment from phosphate or iron oxide sources (MREE/MREE*):

$$BSI = \frac{2 * ([Sm]_{SN} + [Gd]_{SN} + [Dy]_{SN})/3}{([La]_{SN} + [Pr]_{SN} + [Nd]_{SN})/3 + ([Ho]_{SN} + [Er]_{SN} + [Tm]_{SN} + [Yb]_{SN} + [Lu]_{SN})/5}$$

(4)

Other possible contaminants are Mn oxides and hydroxides, which contain a reduced Y anomaly and a positive Ce anomaly compared with ambient waters (Fig. 1; Bau and Dulski, 1996). Fe (oxyhydr)oxides often contain a MREE-enriched signal, with more pronounced Y depletion than Mn (oxyhydr)oxides (Bau et al., 2014; Haley et al., 2004). The significance of contamination from Fe oxides is difficult to ascertain due to their often similar REY patterns, and Fe concentrations are rarely reported alongside REY data for carbonates (Bau et al., 2014). Volcanic ash could also act as a contaminant in some sedimentary settings (Zhou et al., 2000). Organic matter can also carry REY, in some cases with a seawater signature, and authigenic carbonate formed at hydrocarbon seeps records anomalous pore water REY (Freslon et al., 2014; Hu et al., 2014). The assessment of the quality of the REY data is based on the assumption that the REY composition of ancient seawater should resemble modern seawater. But this may not have been the case in ancient oceans (see discussion in Shields and Webb, 2004). This is of particular concern for Precambrian samples (>541 Ma), when the concentration of anions in seawater may have been very different; the distribution of REY is primarily controlled by complexation with anions such as $CO_3^{2-}$ and $SO_4^{2-}$ (Möller and Bau, 1993).

There is variability in the method used for carbonate dissolution in REY studies in the literature, including using nitric acid of varying strength (Bodin et al., 2013; Meyer et al., 2012; Nothdurft et al., 2004; Webb and Kamber, 2000), acetic acid (Ling et al., 2011; Nothdurft et al., 2004; Tessier et al., 1979), buffered sodium acetate solution (Tessier et al., 1979) or hydrochloric acid (Banner et al., 1988; Shields et al., 1997). The dissolution step is performed for varying lengths of time, and sometimes at high temperature (Bodin et al., 2013). Most studies leach the sample in one-step, or in some cases two, using different acids (Meyer et al., 2012; Tessier et al., 1979). Different leaching procedures may preferentially attack different components of the whole rock, such as early and late carbonate cements, dolomite, organic matter, clays and oxides. Sequential leaching experiments have resulted in improvements in the strontium isotope method (Bailey et al., 2000; Li et al., 2011), but carbonates have not been fully assessed for how the REY signature evolves throughout the leaching process as different components dissolve at differing rates and contribute to the final signature (see Zhang et al., 2015 for existing work). Here, we systematically compare REY patterns in sequential leaches in nitric acid from 195 modern and ancient carbonate samples from a wide range of environments, as well as the effect of different acid types and strengths. We also compare Ce anomalies with Fe-speciation data (Clarkson et al., 2014; Wood et al., 2015). Both redox proxies are calibrated for use in carbonate sediments, but have different limitations. Fe-speciation breaks down the relative proportion of $Fe_T$ in the form of carbonate Fe, Fe oxides or siliciclastics, which all have unique REY signals, and hence can help to identify sources of contamination.

## 2. Methods

### 2.1. Samples

Samples of varying purity were collected from a range of modern and ancient settings (Clarkson et al., 2014; Wood et al., 2015), and some are partially or fully dolomitised. For all samples the weathered surfaces were

removed and the carbonate was ground to a fine powder using a diamond tipped drill, or an agate TEMA mill after removal of weathered edges.

Carbonates from the Zhaowei Formation, Huaibei Region on the north China craton, were likely deposited during the Tonian Period (Xiao et al., 2014). These samples were used for leaching experiments alongside reference materials CRM 1c and CRM 88a (an argillaceous limestone and a dolomite, respectively). The majority of the samples are from the Kanies and Omkyk members of the Kuibis Subgroup, Nama Group, deposited in the Zaris Basin ~550–547 Ma (Wood et al., 2015). These sections span four localities from deep outer ramp (Brak), deep inner ramp (Zebra River and Omkyk) and shallow inner ramp (Zwartmodder) settings, and are all very pure carbonates (>> 85% CaCO$_3$). Fe-speciation data for all samples from the Nama Group is included in the online supplementary dataset, with further details available in Wood et al. (2015). Brak consists of mixed limestones and dolomites with low siliciclastic components, which were used for sequential leaching experiments. Zwartmodder and Zebra River sections contain pure limestones and subordinate dolostones, and were used to compare dissolution in acetic and nitric acid. Selected samples from Omkyk section, Nama Group, were used for sequential leaching, as well as single step dissolutions in both acetic and acetate buffer solution.

Samples from the Majiatun, Cuijiatun and Xingmincun Formations in the Dalian area were deposited on the North China Craton during the Tonian Period. These samples were used for comparing the effects of dissolution in different acids. Seven limestones from shallow shelf facies in the Doushantuo Formation, the Dengying and the Yanjiahe Formations in the Yangtze Gorges area, South China, deposited ~635–551 Ma (see Ling et al., 2011 for more details), were leached in nitric acid and acetate buffer solution.

New REY data are presented for modern carbonate samples from a diverse range of oxic and anoxic environments, previously analysed for Fe-speciation, TOC and %CaCO$_3$ (see Clarkson et al., 2014 for full details of samples and previous data). These include pure biogenic carbonates, ooids and carbonate sands from temperate and tropical environments, including shallow marine carbonate platforms. Samples from a restricted environment (AD$xx$) have undergone early recrystallisation and dolomitisation. One additional sample, MCS, is a modern cool water coral carbonate sand with benthic foraminiferans, collected from Achiltibuie Beach, NW Scotland.

## 2.2. Rare earth elements

Table 1 summarizes the samples used in each procedure in this study. All samples were analysed on a Bruker M90 ICP-MS in the Cross-Faculty Elemental Analysis Facility, University College London, and run against multi-element matrix matched standards within an appropriate concentration range. Oxide interference was monitored using formation rate of Ce oxide and the formation of 2 + ions was monitored using Ba$^{2+}$. All REY concentrations were normalized to post-Archean Australian Shale (PAAS: Taylor et al., 1981; Pourmand et al., 2012). All acids used in this study were trace metal grade and concentrations are reported as weight-to-volume ratios. Standard solutions analysed after every ten samples were within 5% of known concentrations. Replicate analyses on the ICP-MS give a relative standard deviation <5% for most trace elements, with a larger standard deviation for the heavy REE that sometimes have non-normalized concentrations <0.5 ppb. Carbonate standard material CRM 1c was prepared using the same leaching procedure as the samples, and repeat analyses give a relative standard deviation <5% for individual REY concentrations, and calculated Ce anomalies (average = 0.80) give a relative standard deviation <3%.

### 2.2.1. Sequential leaching

Three-stage sequential leaching was performed on dolomite and calcite samples from Brak ($n = 14$ dolomite, $n = 11$ calcite) and Omkyk ($n = 5$ calcite), CRM 1c and 88a and Zhaowei Formation carbonates. Powdered carbonate samples were cleaned in deionized water, and

**Table 1**
Summary of samples, procedures and acid type used throughout this study.

| Samples | Procedure | Acid (w/v) |
|---|---|---|
| Zhaowei, CRM, Brak, Omkyk | Sequential leaching in 3 stages | 2% nitric |
| Zebra River, Dalian, Zwartmodder, Omkyk | Partial leach | 2% nitric |
| | Single step digestion | 2% acetic |
| CRM, Omkyk, Zebra River, Yangtze Gorges | Single step digestion | Acetate buffer sol. |
| Modern sediments | Sequential leaching in 5 stages | 2% nitric |
| | Single step digestion | 2% nitric |
| | | 2% acetic |
| Modern sediments | Fe-speciation (Clarkson et al., 2014) | |
| Brak, Zebra River, Zwartmodder | Fe-speciation (Wood et al., 2015) | |

then a sufficient number of moles of 2% nitric acid to dissolve 20% of the sample (based on a theoretical purity of 100% CaCO$_3$) were added dropwise. The sample was agitated on a shaker for 20 min at room temperature before being centrifuged. The supernate was removed and the solution was made up to 10 ml of 2% nitric acid for analysis. The procedure was then repeated twice, but each dissolving 40% of the sample, until sufficient acid to dissolve 100% of a pure carbonate sample had been added. Samples were leached in three stages: a first leach, 0–20%, a central leach, 20–60%, and a final leach, 60–100%. Single-step sample dilutions in excess 2% nitric acid were prepared for comparison.

### 2.2.2. Comparing acids

Samples from Dalian, Zebra River ($n = 67$ calcite, $n = 2$ dolomite), Zwartmodder ($n = 8$ dolomite, $n = 31$ calcite), Omkyk ($n = 6$ calcite) and CRM 88a and 1c were digested in a single step using acetic acid to compare with a nitric central leach. Samples were dissolved in 2% acetic acid and shaken for 20 min. The supernate was transferred, dried down in an oven, washed twice in 50% nitric acid and resuspended in 2% nitric acid for analysis. Single step digestions in 2% acetic acid from Zwartmodder were analysed in an acetic matrix to compare the matrix effects of nitric and acetic acid within the ICP-MS, since analysing in an acetic acid matrix may lead to interferences with acetate complexes.

A range of samples showing positive and negative Ce anomalies in a nitric partial leach, Omkyk ($n = 6$ calcite), Zebra River ($N = 7$ calcite), were also dissolved in a pH 4.5 sodium acetate buffer solution in order to compare with a method commonly used for selective carbonate dissolution in other geochemical protocols, e.g. Fe speciation (Poulton and Canfield, 2005). After shaking for 48 h, the supernate was then transferred into a new vial and dried in an oven, washed twice in 50% nitric acid and suspended in 2% nitric acid for analysis.

### 2.2.3. Modern sediments

New REY data are presented for modern carbonate samples from a diverse range of environments (Clarkson et al., 2014), to investigate REY patterns in carbonates deposited beneath oxic and anoxic water columns. The samples were leached in five stages using 2% nitric acid, each designed to dissolve 20% of the sample (based on a theoretical purity of 100% CaCO$_3$), as well as a single step digestion in both 2% nitric and 2% acetic acid, to test different leaching procedures on unlithified sediments.

## 2.3. Major elements

Carbonates prepared for REY analysis were also analysed for major element concentrations (Ca, Mg, Fe, Al and Sr) using an ICP-OES in the Cross-Faculty Elemental Analysis Facility, University College London, to identify dolomitisation, recrystallization and carbonate content. Total digestions of samples from Zebra River, digested using HNO$_3$–HF–B(OH)$_3$–HClO$_4$ at the University of Leeds, were resuspended in a 2% nitric acid matrix and additionally analysed for Ba, K, Zr, P, Ti and Si. Samples were screened for dolomitisation using Mg/Ca ratios.

## 2.4. Fe-speciation

Fe speciation data for carbonates discussed here come from previously published data (Clarkson et al., 2014; Wood et al., 2015). The Fe-speciation technique was performed using well established sequential extraction schemes (Poulton and Canfield, 2005). The method targets operationally defined Fe pools, including carbonate-associated-Fe ($Fe_{Carb}$), ferric oxides ($Fe_{Ox}$), magnetite ($Fe_{Mag}$), pyrite Fe ($Fe_{Py}$) and $Fe_T$. $Fe_{HR}$ refers to Fe minerals that are highly reactive towards biological and abiological reduction under anoxic conditions, and is defined as the sum of $Fe_{carb}$ (extracted with Na-acetate at pH 4.5 and 50 °C for 48 h), $Fe_{ox}$ (extracted via Na-dithionite at pH 4.8 for 2 h), $Fe_{mag}$ (extracted with ammonium oxalate for 6 h) and $Fe_{py}$ (calculated from the mass of sulfide extracted during $CrCl_2$ distillation). $Fe_T$ extractions were performed on ashed samples (8 h at 550 °C) using $HNO_3–HF–B(OH)_3–HClO_4$. All Fe concentrations were measured via atomic absorption spectrometry and replicate extractions gave a RSD of <5% for all steps.

Calibration in modern and ancient marine environments suggests that $Fe_{HR}/Fe_T < 0.22$ indicates deposition under oxic water column conditions, while $Fe_{HR}/Fe_T > 0.38$ indicates anoxic conditions. Ratios between 0.22 and 0.38 are considered equivocal, and may represent either oxic or anoxic depositional conditions. The nature of anoxia is determined by the extent of sulphidation of $Fe_{HR}$, whereby $Fe_{py}/Fe_{HR} > 0.8$ is diagnostic for euxinic conditions, whereas $Fe_{py}/Fe_{HR} < 0.7$ defines ferruginous deposition.

These thresholds are also applicable to carbonate-rich sediments that have not undergone late stage dolomitisation (Clarkson et al., 2014), on the condition that $Fe_T > 0.5$ wt%. The primary concerns for the use of Fe-speciation in carbonate-rich sediments are related to the decreased detrital components, and hence low $Fe_{HR}$ and $Fe_T$. This can increase the sensitivity of the proxy to $Fe_{HR}$ inputs that are unrelated to the anoxic water column formation of $Fe_{HR}$ minerals, as might occur during early diagenesis. The impact of this process has been demonstrated to be less significant when $Fe_T > 0.5$ wt% (Clarkson et al., 2014), where carbonate-rich sediments may behave in a manner that is consistent with shales.

## 3. Results

### 3.1. Sequential leaching

Carbonate rocks leached in three stages in nitric acid show a clear and consistent evolution in REY patterns with each sequential leach (Fig. 2). Low bell shaped index, low $\sum$REE (sum concentration of each shale normalized REE, in ppb) and high Y/Ho ratios (>36) all indicate a low degree of contamination from non-carbonate phases, and these parameters were used to assess the purity of each leach. Eu anomalies can result from hydrothermal activity but small anomalies may result from clay contamination, or oxide interferences, and so small Eu anomalies (<1.5) may also indicate minimal contamination.

There is a clear distinction between the leaching behaviour for calcite and dolomite (figs. 2 and 3). For calcitic rocks, the first leach (0–20%) shows flat patterns with Eu anomalies that lack seawater characteristics, and have low concentrations of REY in solution. For all calcite samples the central leach (20–60%) produces the most seawater like REY patterns, as shown by a lower BSI, higher Y/Ho, lower $\sum$REE, more positive La anomalies and higher $Yb_{SN}/Nd_{SN}$ than the final leach. A full, single step digestion of calcite in nitric acid results in similar patterns to the first leach, with lower REY concentrations than sequential leaches. This suggests that REY are lost from solution during the first acid treatment, even with sufficient moles of acid to take the reaction
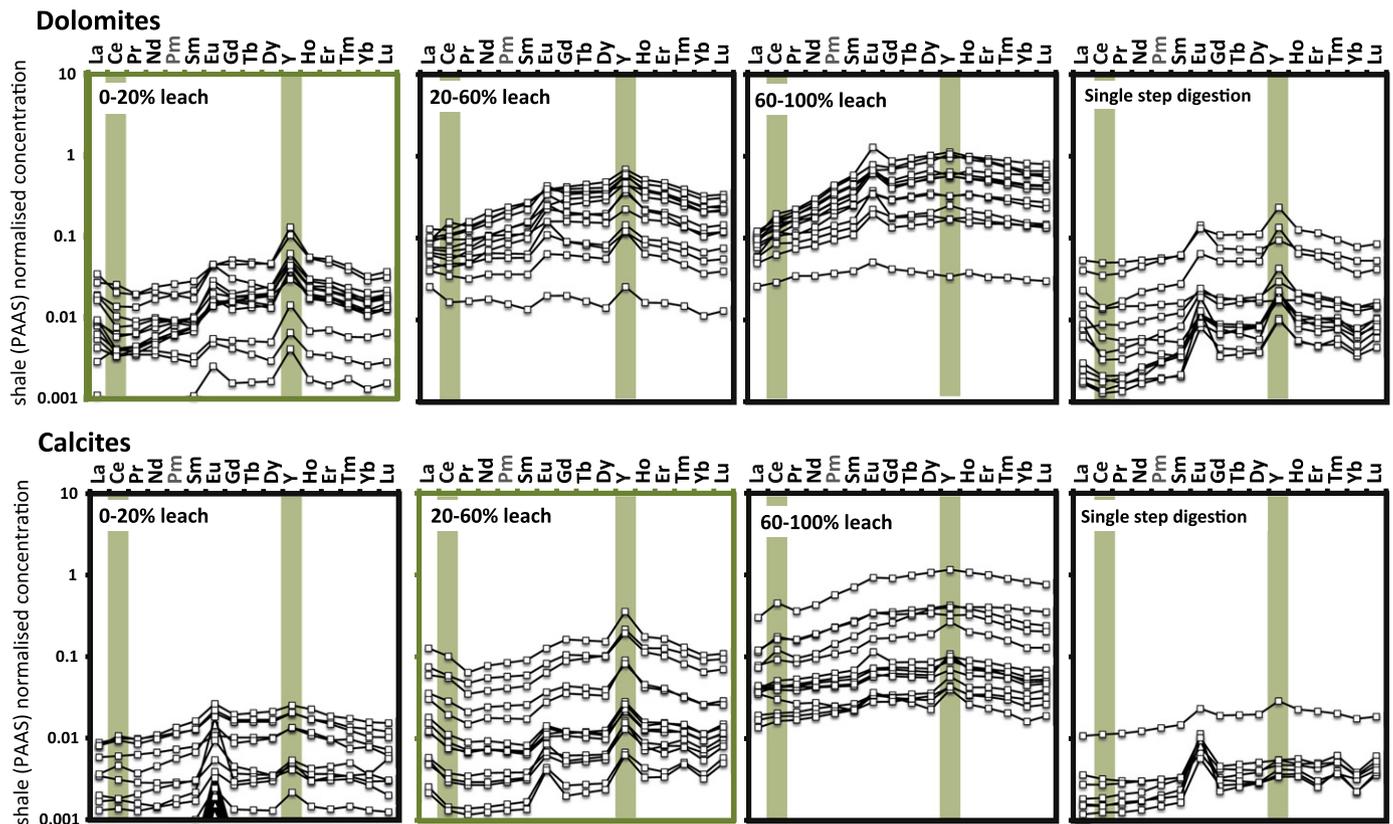


**Fig. 2.** REY patterns for dolomite and calcite for sequential leaches in 2% nitric acid. The first 20% leach, the second 40% leach and the third 40% leaches are shown for both calcitic and dolomitic samples from Brak, samples from Zhaowei, and selected samples from Omkyk. A single step digestion in nitric acid is shown for comparison. The scale is consistent between plots for ease of comparison, with shale-normalized concentrations below 0.001 omitted as associated non-normalized concentrations are commonly below the detection limit of the ICP-MS. The patterns evolve with each sequential leach, with optimal seawater conditions reached in the first leach for dolomites and the central leach for calcites (green box). Green bars highlight important REY, Ce and Y. Theoretical Pm values are calculated as $(Nd_{SN} + Sm_{SN})/2$.
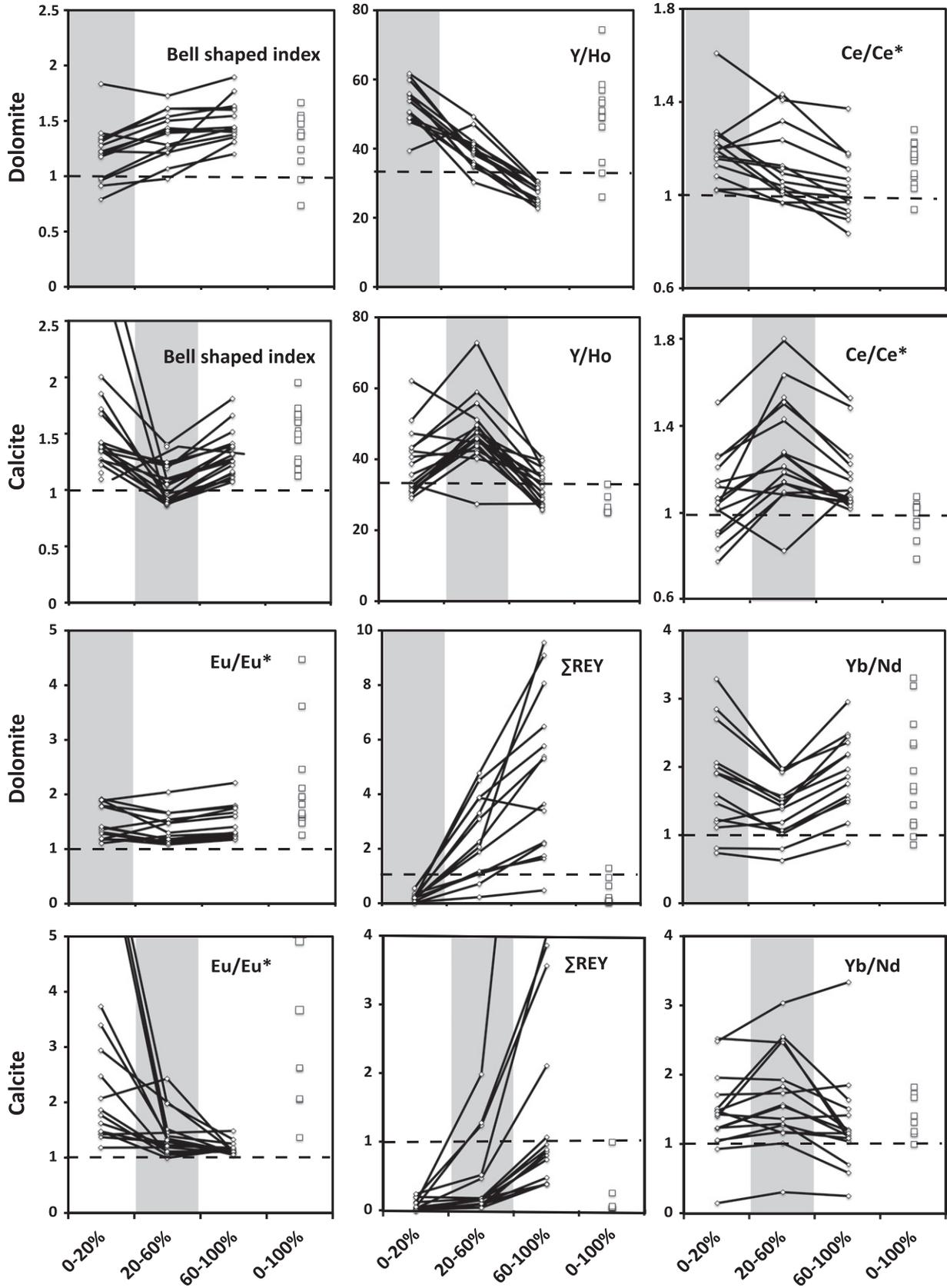
**Fig. 3.** Sequential leaching patterns for both dolomite and calcite in 2% nitric acid. Key comparative parameters of bell shaped index, Y/Ho, $Ce_{SN}/Ce_{SN}*$, $Eu_{SN}/Eu_{SN}*$, $\sum REE$ and $Yb_{SN}/Nd_{SN}$ are shown for the first 20% leach, the central 40% leach and the final 40% leach for both calcitic and dolomitic samples from Brak, Zhaowei, and selected samples from Omkyk. A full digestion in nitric acid is shown for comparison (open squares). Dashed lines indicate key thresholds for each parameter. The patterns evolve with each sequential leach, with optimal seawater conditions reached in the first leach for dolomites and the central leach for calcites (grey bars).

to completion. For dolomitic samples it is the first leach that shows less deviation from an expected seawater pattern. A single step digestion gives similar results. The central and final leaches have higher $\sum$ REE, lower Y/Ho, reduced La anomalies and a higher BSI. The leach with the clearest seawater characteristics for both dolomite and calcite samples is associated with the most pronounced Ce anomaly, regardless of whether the anomaly is positive or negative. A single-step digestion would reduce the magnitude of any Ce anomaly in calcite samples.

Ba and P contents of full digestions for Zebra River show no correlation with Y/Ho ratios recorded for a central leach in nitric acid (Fig. 4). Ti, Zr, Al, Fe and K concentrations, however, are higher in samples where the central leach does not contain a Y anomaly > 36, consistent with clay leaching contaminating the authigenic REY signal from the carbonate inventory. Additionally, Ba/Sm ratios show no correlation with $Eu_{SN}/Eu_{SN}{}^*$, as would be expected if Eu anomalies were resulting from interference within the ICP-MS. P contents are low and show no correlation with BSI, indicating that predictable effects of leaching from diagenetic phosphates can be neglected in these samples.

### 3.2. Acid comparison

A single step dissolution in acetic acid produces distinct REY patterns compared with the same samples partially leached in nitric acid (Fig. 5), and these results are consistent regardless of whether analysis is conducted in an acetic or nitric acid matrix. A single step dissolution in acetic acid consistently results in weaker La and Y anomalies and higher $\sum$ REE (Fig. 6). While Mn concentrations are similar for nitric partial leaches and acetic single step leaches, Fe and Al contents are higher in acetic single step leaches (Fig. 6), which would be best explained by the partial leaching of clay minerals.

Sodium acetate buffer solution, mediated by acetic acid, is maintained at a pH of 4.5. Acetate buffer is used to selectively dissolve carbonate in a range of geochemical studies (Tessier et al., 1979) and should in theory result in a pure REY leach sourced from the carbonate portion of the sample. In particular, acetate buffer solution is used during the Fe-speciation sequential extraction procedure to isolate Fe from carbonates, without leaching Fe oxides, magnetite or clays (Poulton and Canfield, 2005). Acetate buffer was used here to leach samples in a single step, targeting samples with positive and negative Ce anomalies, and results in REY patterns with weak La and Y anomalies and higher $\sum$ REE compared with nitric partial leaches. Ce anomalies are present using both methods, but are more pronounced in nitric partial leaches (Fig. 7).

### 3.3. Modern samples

Modern carbonate sediment samples from a range of environments (Clarkson et al., 2014) were leached in five stages in 2% nitric acid, as well as single-step digestions in both 2% nitric and 2% acetic acid. For
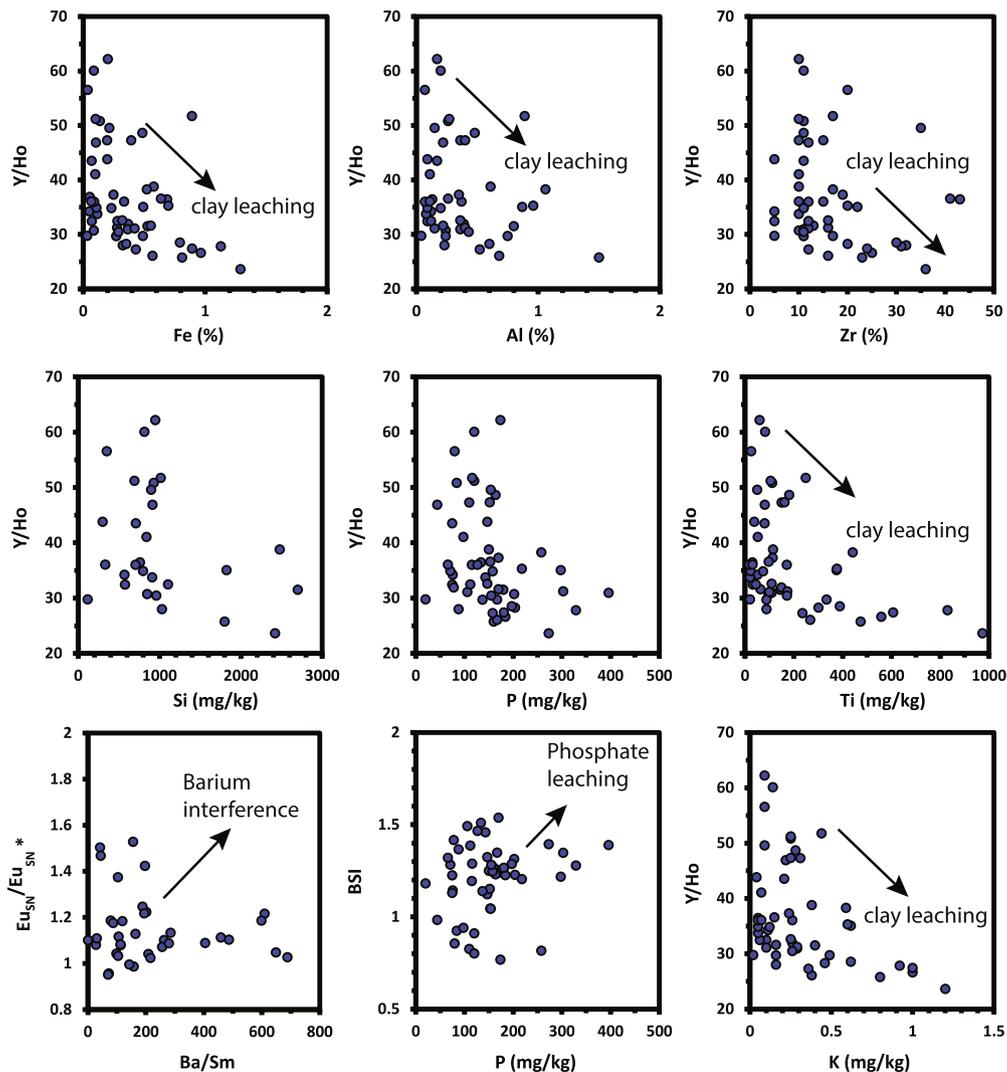


Fig. 4. Ba P, Ti and K contents of full digestions for Zebra River compared with REY parameters recorded in a central leach in nitric acid. Ba shows no correlation with $Eu_{SN}/Eu_{SN}{}^*$. P shows no correlation with BSI. Samples with higher Y/Ho ratios show lower Ti and K in general, but no correlation with P or Ba/Sm.
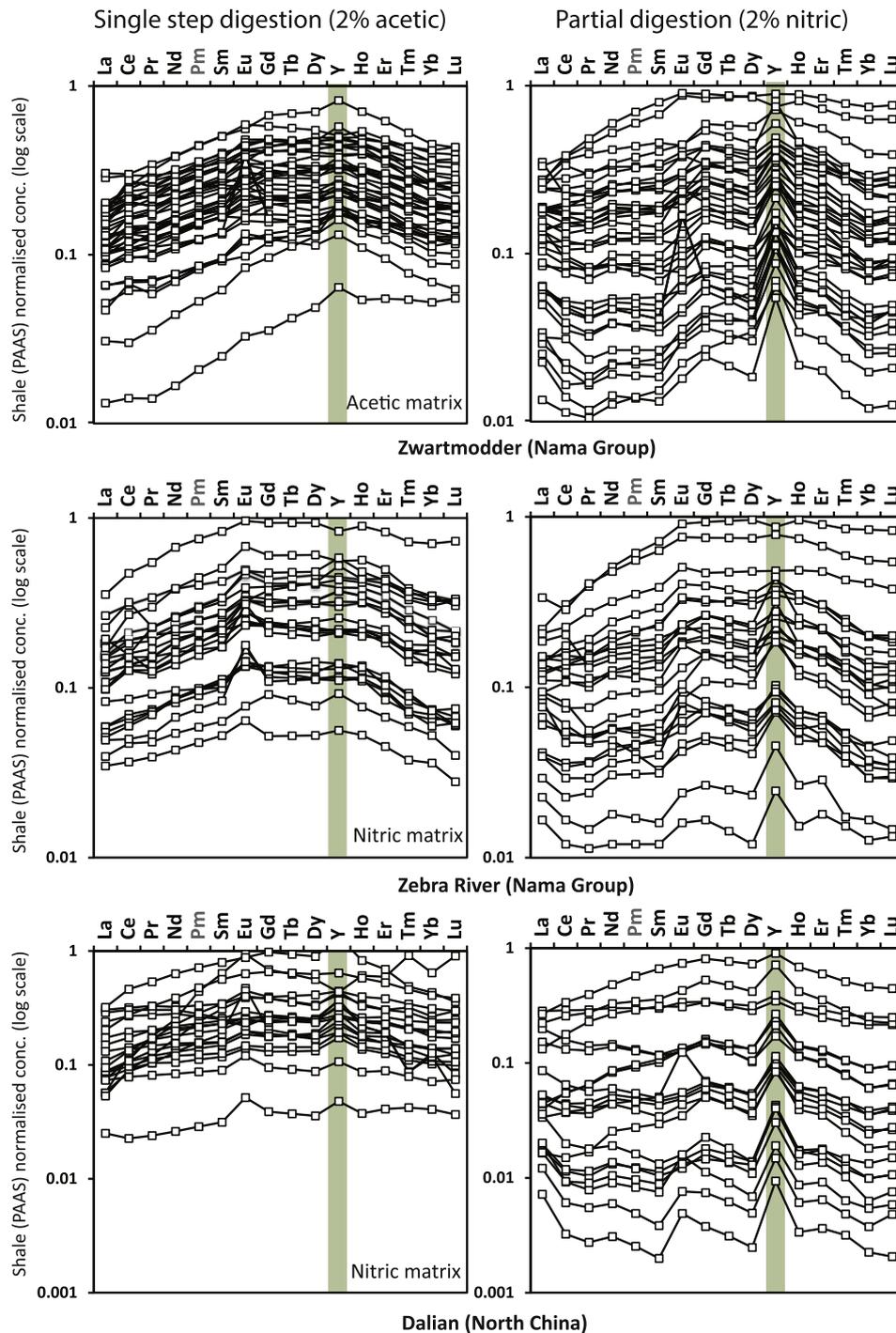
**Fig. 5.** Comparative REY patterns for samples dissolved in 2% acetic acid and for a partial leach in 2% nitric acid from various sites. Partial dissolution in nitric acid consistently results in larger Ce and La anomalies, larger Y anomalies (highlighted by green bar) and lower $\sum$ REE than for a single-step digestion of the same sample in acetic acid. The matrix used for ICP-MS analysis is indicated for the acetic single-step leaches. Theoretical Pm values are calculated as $(Nd_{SN} + Sm_{SN})/2$.

impure carbonates (below 85% $CaCO_3$) REY patterns are often dominated by clay signals, and in general, earlier leaches result in more seawater like REY patterns for impure carbonates (Fig. 8 and Table 2). Optimal leaches for each sample have been selected based on the closest resemblance to seawater patterns, using Y/Ho as the primary discriminator (see Fig. 9). As well as the purity, the sediment type appears to have a significant effect on the REY pattern of the targeted carbonate fraction. Carbonate slope sediment, temperate carbonate sands, some inter-reef carbonate sands, temperate shallow water limestone, carbonate ooze and anoxic deep water carbonate appear to accurately record features of seawater REY, along with appropriate Ce anomalies for the redox

environment. However, ooids, some inter-reef carbonate sands, dolomites from sabkha environments, and organic rich microbial carbonate and some skeletal carbonate do not record appropriate Ce anomalies or other seawater REY features, or have been contaminated with non-carbonate phases during leaching. The three anoxic samples show no Ce anomaly using any leaching method, as expected.

### 3.4. Identifying sources of contaminant REY using Fe-speciation data

A pure carbonate leach should record pristine seawater REY patterns, including a positive Y anomaly. Here, we are concerned with
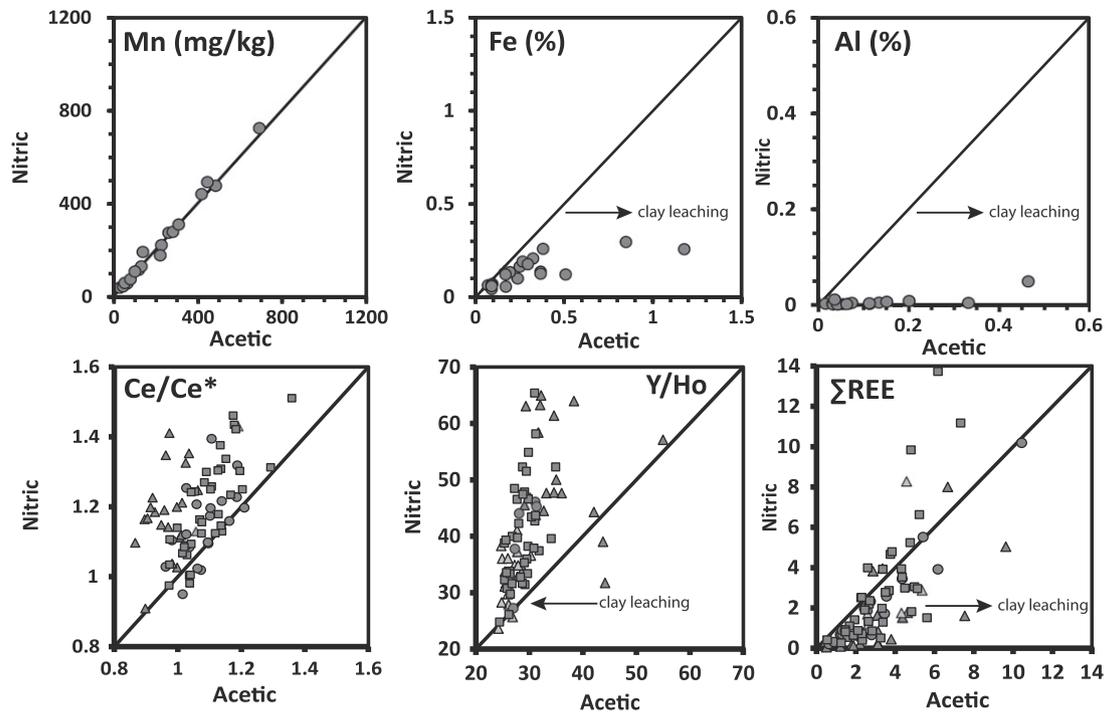
**Fig. 6.** Cross plots of major elements and REY parameters for samples dissolved in a single step in 2% acetic acid and for a partial leach in 2% nitric acid (20–60% fraction) from Zwartmodder (squares), Zebra River (circles) and Dalian (triangles). Dissolution in nitric acid results in larger Ce anomalies, more positive Y anomalies and lower $\sum$REE than for the same sample dissolved in acetic acid. Dissolution in acetic acid leaches more Fe and Al than a partial leach in nitric acid, indicating clay leaching.

whether the acid is attacking primary depositional carbonate or additional phases such as clays, which have no Y anomalies, or Fe-Mn (oxyhydr)oxides, which may host the complementary scavenging signal to the seawater signal with negative shale normalized Y anomalies.

Sections from the Nama Group have been used to compare REY patterns from nitric acid central leaches with Fe-speciation data (Wood et al., 2015). The $Fe_T$ is composed of Fe originating from both clays (approximated as poorly reactive Fe, $Fe_{PR}$, and unreactive Fe, $Fe_{UR}$), and Fe species that are highly reactive to abiological reduction under anoxic conditions ($Fe_{HR}$). Highly reactive Fe is predominantly in the form of Fe oxides and carbonate Fe in all samples considered here, and magnetite Fe and pyrite concentrations are low (see online supplementary data set). The concentration of Fe measured in REY partial leaches is lower than $Fe_T$, and in general, is likely to be composed predominantly of Fe carbonate phases.

In general, the Y anomaly is more pronounced in samples with low $Fe_T$ (Fig. 10A). For samples with >0.5 wt% $Fe_T$, a breakdown of the Fe phases is available from Fe-speciation data (Fig. 10B). When the Y anomaly is compared with the concentration of different types of Fe in the whole rock, a distinct pattern emerges. Samples with higher clay components are associated with lower Y anomalies, reflecting the increased likelihood of partial clay leaching. Clay minerals contain high concentrations of REY with flat detrital patterns, which would dilute any Y anomaly originating from the carbonate phase. The contribution of clays is likely higher in samples with low %$CaCO_3$, which are also prone to higher $Fe_T$. The use of Y anomalies to screen for clay leaching is further supported by the reduced Y anomalies in leaches with high concentrations of K, Ti, Zr and Al (Fig. 4).

Y anomalies are unaffected by the concentration of carbonate Fe, which is to be expected as the Fe hosted within carbonate is not associated with an independent REY reservoir. Where the Fe oxide content is high (>0.1 wt%), Y anomalies are low (<36) for 75% of the samples. This indicates that Fe oxides, where present, may be dissolved during a partial leach in nitric acid and affect the REY signal, and this can be identified and addressed through imposing a threshold value for Y/Ho ratios of >36. This also implies the Fe oxides host a non-seawater REY pattern with low Y anomalies, which is consistent with some REY fractionation

during adsorption onto Fe (oxyhydr)oxides (Bau et al., 2014; Haley et al., 2004).

## 4. Discussion

### 4.1. Leaching procedure

Dissolution of limestone in acid is complex, with different components such as early cements, late diagenetic cements, dolomite, kerogen, phosphates, clays and Fe-Mn (oxyhydr)oxides dissolving at different rates and pH ranges. It is therefore unsurprising that sequential leaching experiments show clear patterns for the evolution of the REY pattern throughout dissolution. The first leach will include adsorbed ions and easily exchangeable ions associated with clay minerals. The first leach gives poor results for calcitic samples in our study, and we recommend a pre-leach (20% of the sample) that is then discarded. The low concentration suggests REY are not coming into solution from the phases that initially react with acid. However, since single step digestions in excess acid shows similarly low-concentrations, REY must be coming into solution, but then readsorbing to the walls of the vial or the solid residue (Sholkovitz, 1989). The 'sticky' properties of REY in an acidic solution, and any fractionation that may occur during this process, are poorly constrained and require further attention. This potential adsorption may present a problem, if there is dynamic exchange between adsorbed and freshly dissolved ions during subsequent leaching. We therefore suggest the residue is rinsed three times in ultrapure water between leaching steps.

The central leach shows the closest resemblance to modern seawater patterns, and the major elements indicate the lowest degree of contamination from non-carbonate phases. We suggest that this is because calcite is likely to dissolve early, with the final leach attacking non-carbonate phases such as clays and oxides. Therefore, dissolution in excess acid would result in higher contributions from non-carbonate phases. Based on our study, for calcite samples we recommend sequential leaching in 2% nitric acid, and retention of the central leach for analysis in a nitric acid matrix as best practice (Fig. 11). Samples from different settings may respond differently to leaching, and so preliminary tests,
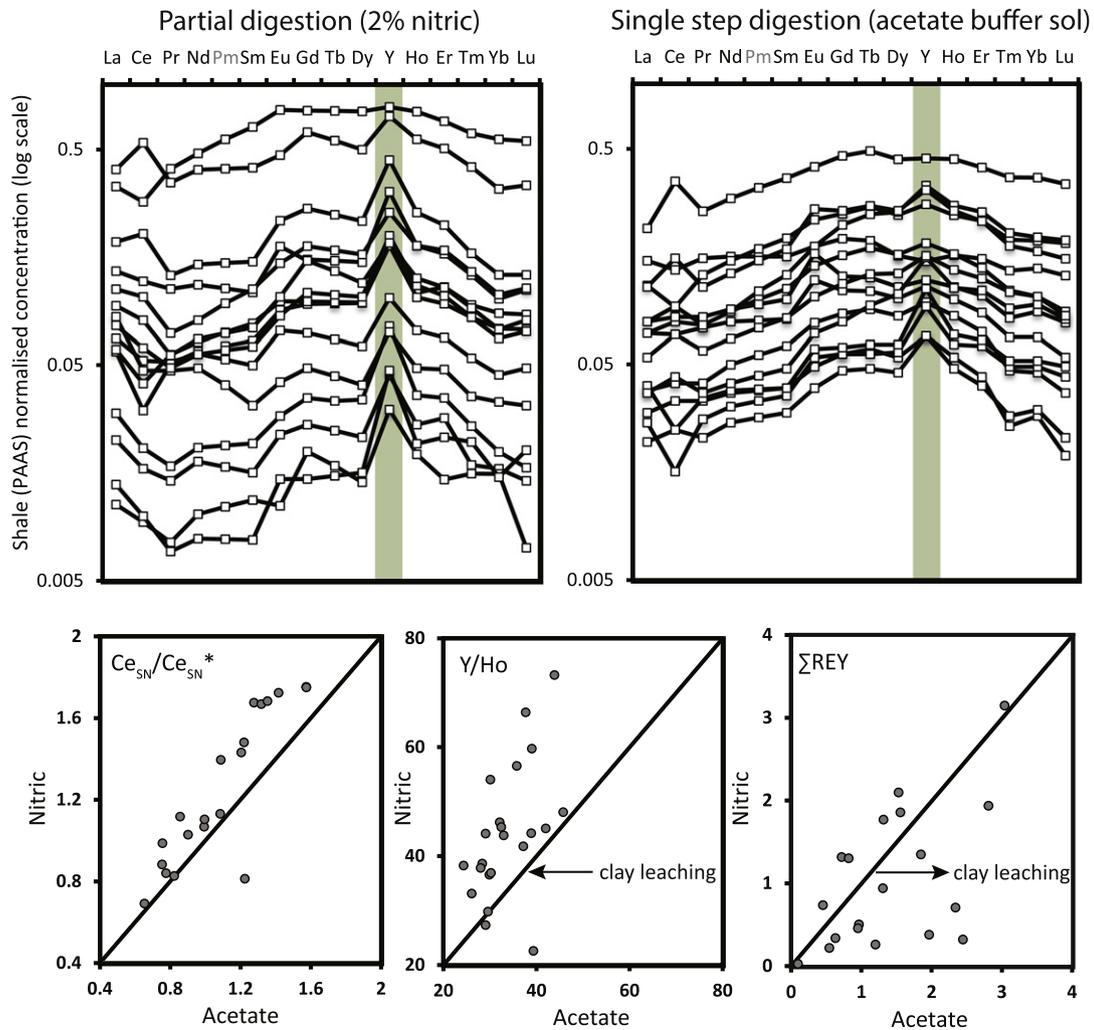
**Fig. 7.** Cross plots of REY parameters and REY patterns for samples dissolved in pH 4.5 sodium acetate buffer solution and for a partial leach in 2% nitric acid from various sites. Dissolution in nitric acid results in more positive Y anomalies and lower $\sum$ REE than for the same sample dissolved in acetate buffer. Cerium anomalies are detected with both methods. Theoretical Pm values are calculated as $(Nd_{SN} + Sm_{SN})/2$.

similar to those described here, should be performed to identify best practice before a full stratigraphic REY study.

We have not tested the effects of leaching in hydrochloric acid. Although HCl is a poor matrix material for ICP-MS analysis, the sample may be digested in HCl and resuspended in nitric acid, as demonstrated for acetic leaches here. We have compared the effects of a single step digestion in acetic acid, and partial leaching in nitric acid (Figs. 5 and 6). Acetic acid is considered to be gentler than nitric acid, because the hydrogen ions do not fully dissociate in water, especially at higher concentrations. Acetic is a reducing acid whereas nitric is oxidising, and hence nitric acid may preferentially attack various mineral phases, such as organic matter or sulfide minerals (Analytical Methods Committee, 1960). For these reasons, acetic acid has been preferred in REY studies, on the assumption that it should only leach carbonate without attacking other phases (Ling et al., 2011; Nothdurft et al., 2004; Tessier et al., 1979). However, when dilute, acetic acid acts like a strong acid and should be at least as aggressive as nitric acid.

The relative dissolution rates of $CO_3^{2-}$ and clay minerals are pH dependent (Chou et al., 1989; Knauss and Wolery, 1989). It is common to maintain solutions above pH 4.5 during selective carbonate dissolution (Tessier et al., 1979). In a pure carbonate digestion the acetic acid can self-buffer due to the increased alkalinity, and may tend towards pH >4.5, similar to sodium acetate buffer solution. However, the high Al contents and REY patterns in single step digestions in acetic acid in this study suggest that acetic acid is leaching additional REY from clays. The single step acetic acid

solutions may still be acidic at the end of the leaching, and so the excess acetic will continue to attack other phases. Here, we present partial leaches in nitric acid, which give less contaminated results, as solutions should be pH-neutral at the end of leaching. We show that a partial leach in nitric acid can give seawater-like patterns, which we assume to come from a pure carbonate leach. Zhang et al. (2015) show a similar evolution pattern of the sequential leach using acetic acid to the one we note here using nitric acid. They also find that a full dissolution in excess 10% or 5% acetic acid results in a contaminated signal. Their results are broadly consistent with ours. Both studies show that a partial leaching is preferable, and that single step digestions result in the leaching of non-carbonate phases such as clays.

REY patterns from leaching in sodium acetate buffer solution (pH 4.5), used during the Fe-speciation procedure to isolate carbonate Fe, suggest that clays are partially leached during this procedure. This would have implications for the Fe-speciation technique if significant amounts of Fe from clays are inadvertently included in the calculation of carbonate Fe, which may affect the calculated ratio of $Fe_{HR}/Fe_T$. However, since clays contain REY concentrations an order of magnitude higher than carbonates, leaching of only a small amount could overwhelm the resulting REY pattern, without resulting in a significant difference in Fe concentrations. The additional Fe leached with sodium acetate buffer solution is likely minor and within the margin of error expected during Fe-speciation sequential extraction (Poulton and Canfield, 2005) (see Fe concentrations in Fig. 6).

Extremely large water:rock ratios are required to alter the REY signature of diagenetic carbonate, and so dolomites are thought to
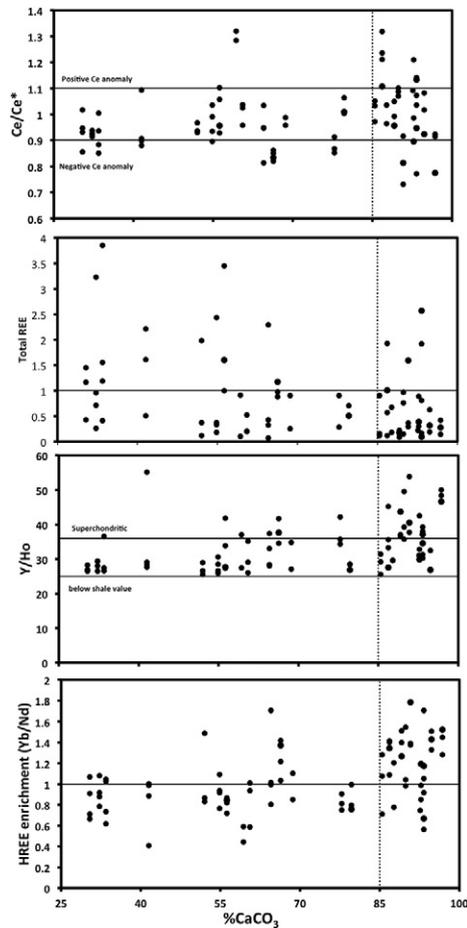
**Fig. 8.** %CaCO$_3$ against three key REY parameters (Ce$_{SN}$/Ce$_{SN}$*, Y/Ho and Yb$_{SN}$/Nd$_{SN}$) for modern samples. All data within the detection limit of the ICP-MS is shown, including leaches 1 to 5 in 2% nitric acid, and single step digestions in 2% nitric and 2% acetic acid. The parameters show an increase in quality above 85% purity.

preserve the same seawater REY signatures as co-occurring carbonates (Banner et al., 1988). Furthermore, Zhang et al. (2015) show that leaches containing a higher proportion of Mg (presumed to be from dolomite dissolution) are consistent with REY patterns in calcite. Dolomite reacts an order of magnitude more slowly with acid than calcite at pH 4.5 (Chou et al., 1989), and so the first leach may attack the calcite portion of the rock, with later leaches attacking the dolomitic portion. In our study, early leaches contain a more pristine seawater REY signal for partially dolomitized samples, and we suggest that this is because the calcite phase dissolves earlier. Once the calcite phase is exhausted, dolomite may begin to dissolve, resulting in leaches showing higher REY concentrations and reduced Y anomalies. This suggests that either dolomite does not record pristine seawater REY patterns, or that the recalcitrant dolomite phase dissolves at similar rates to non-carbonate phases such as clays. However, calcite phases in calcareous dolostones could be in the form of secondary veins and cements, so targeting the calcitic component of a dolomitic rock is not always recommended. Furthermore, early leaches may also contain adsorbed ions and easily exchangeable ions associated with clay minerals. For the partially dolomitized samples in our study, the optimal procedure is to retain the first 20% leach in 2% nitric acid (Fig. 11). Hereafter, the optimal procedure for dolomites will depend on the individual samples, and should be considered on a case-by-case basis. It may also be important to distinguish between early and late stage dolomitisation. While early dolomitisation may recycle local pore water or seawater REY, there is greater potential for alteration during late stage dolomitisation as higher REY contents would be liberated from siliciclastics at depth (Abanda and Hannigan, 2006; Carmichael and Ferry, 2008; Kahle, 1965).

### 4.2. Modern sediments

The modern sediments presented here are from diverse settings compared to the ancient rocks used in this study and the optimal leaching procedure is less clear. There are some broad patterns: earlier leaches give better results for low purity carbonates, and later leaches give better results for pure carbonates, as the reduced carbonate phase is exhausted earlier in the leaching process. In general, Y anomalies are reduced when the sample is leached in a single step in acetic acid, indicating a greater extent of clay leaching. Many of the modern samples analysed here have low %CaCO$_3$, and so the REY patterns are compromised by partial clay leaching for many samples, particularly for dolomitised samples.

The REY leached from some modern samples do not display pronounced negative Ce anomalies, despite forming in oxic waters. The formation of Ce anomalies depends on the preferential scavenging of Ce(IV) onto sinking insoluble particles throughout the oxidised water column and negative Ce anomalies are ubiquitous in the modern open ocean (Fig. 9). However, ocean margin seawater, and near-shore settings or enclosed bays may exhibit reduced negative Ce anomalies (Johannesson et al., 2006; Nozaki and Zhang, 1995; Zhang and Nozaki, 1998). The absence of negative Ce anomalies in some modern sediments may be a result of their formation in restricted settings where ambient water does not display a pronounced negative Ce anomaly. However, the leaching procedure developed on ancient, pure and organic poor carbonate rocks may be inappropriate for unlithified sediments, skeletal carbonate, impure or dolomitised samples.

Skeletal carbonates are generally pure (high %CaCO$_3$), but they may be precipitated via complex mineralization pathways, and any fractionation effects during this process would be species specific and are poorly constrained. Coral presented here records a positive Y anomaly, but no negative Ce anomaly, consistent with relatively high partition coefficients for Ce during coral growth (Sholkovitz and Shen, 1995), and this may also be the case for other skeletal carbonate samples. Further, REY concentrations are up to ten times lower in skeletal carbonates, and so the dilution factors used here may be inappropriate. REY concentrations fell below the detection limit of the ICP-MS for some leaches, which are likely the most pure carbonate leaches.

Organic rich unlithified material from the top of a stromatolite column in an oxic setting (S unlith; Vasconcelos et al., 2006) shows a distinct REY pattern from other samples, with strong LREE enrichment and modest Y anomalies alongside a positive Ce anomaly. The associated organic matter (>2%) may contain a distinct REY signal, consistent with Freslon et al. (2014), which could be contributing to the leachate. Lithified material from the same stromatolite column (Strom lith) shows a similar non-seawater pattern, but without a significant positive Ce anomaly. Although some microbial carbonates may be good proxies for seawater REY (Webb and Kamber, 2000), there is evidence of REY fractionation during uptake into microbial carbonate (Johannesson et al., 2014) and microbial carbonate may also be associated with ferromanganese crusts. For organic rich carbonate rocks, the use of nitric acid may release REY from organic carbon, and caution should be applied using our leaching method on samples with high TOC.

Carbonate sand and mud samples (AD$xx$, $n = 10$) from a shallow sabkha setting along the restricted coastline of Abu Dhabi have a wide range of purity (30–88%; Clarkson et al., 2014; Lokier and Steuber, 2008). These samples show consistent REY patterns with no negative Ce anomalies and small Y anomalies. The water column in this locality is oxic, but the restricted setting and highly evaporitic environment may preclude Ce anomaly formation (Nozaki and Zhang, 1995; Zhang and Nozaki, 1998). It is likely that the majority of these samples have been affected by partial clay leaching, because of their high siliciclastic contents, and it is possible that for impure samples no leaching procedure is effective enough to extract pure carbonate-bound REY. Further, these samples have undergone early recrystallisation and dolomitisation. The first 20% leach is most effective for dolomite leaching, and hence dolomites are particularly susceptible to contamination during leaching if they are impure. For example, the first 20% leach of a sample

**Table 2**

Fe-speciation, TOC, %CaCO$_3$, Y/Ho and Ce$_{SN}$/Ce$_{SN}$* for modern carbonate samples. The REY data is selected from the optimal leach for each sample, defined as a single step digestion in 2% acetic (A), or sequential 20% leaches, L1 to L5, in 2% nitric acid. %CaCO$_3$, Fe$_T$, Fe$_{HR}$/Fe$_T$, TOC data are from Clarkson et al. (2014). All samples except MCS are from Clarkson et al. (2014). Fe$_{HR}$/Fe$_T$ is reported, but is not applicable in samples with <0.5 wt% Fe$_T$. BD denotes concentrations were below detection. Grey rows are samples from anoxic settings.

| Sample | Description | CaCO$_3$ (%) | Fe$_T$ (%) | Fe$_{HR}$ /Fe$_T$ | TOC (%) | Optimal leach | Y/Ho | Ce$_{SN}$/ Ce$_{SN}$* |
|---|---|---|---|---|---|---|---|---|
| BS ooze | Unit 1 coccolith ooze | 86.86 | 0.441 | 0.74 | 4.46 | L3 | 35.6 | 1.21 |
| BS carb | Authigenic carbonate | 0.696 | 0.67 | 0.28 | L3 | L3 | 28.5 | 1.00 |
| Yazerez | Deep water carbonate/gypsum | 56.25 | 1.598 | 0.54 | 2.48 | L2 | 41.9 | 1.10 |
| MCS | Temperate skeletal carbonate sand | – | – | – | – | L4 | 40.9 | 0.68 |
| GBR 41 | Inter–reef carbonate sands | 96.84 | 0.073 | 1.17 | BD | L4 | 46.6 | 0.78 |
| Pecten | Skeletal carbonate (shell) | 94.77 | 0.014 | BD | BD | L4 | 26.9 | 0.92 |
| Strom. lith | Microbial carbonate | 93.31 | 0.023 | BD | 0.16 | L4 | 37.1 | 1.13 |
| GBR 36 | Inter–reef carbonate sands | 93.31 | 0.439 | 0.85 | BD | L3 | 39.2 | 1.07 |
| Coral | Skeletal carbonate | 92.73 | 0.068 | 1.23 | 0.06 | L2 | 42.5 | 1.20 |
| Coquina | Shelly limestone | 92.62 | 0.021 | BD | BD | L3 | 31.1 | 1.09 |
| Azagador | Temperate shallow water limestone | 90.79 | 0.201 | 0.81 | BD | L4 | 40.5 | 0.81 |
| GBR 38 | Inter–reef carbonate sands | 89.85 | 0.008 | BD | BD | L3 | 49.5 | 1.10 |
| Ooids | Ooids | 89.15 | 0.035 | BD | BD | L4 | 43.7 | 0.96 |
| AD B14 | Dolomitised sabkha ramp sands & mud | 87.68 | 0.641 | 0.34 | BD | L3 | 29.5 | 0.96 |
| AD B15 | Dolomitised sabkha ramp sands & mud | 85.42 | 0.085 | 0.62 | BD | L2 | 31.4 | 1.05 |
| N.Uist 6 | Temperate carbonate sands | 77.84 | 0.648 | 0.36 | 0.12 | L3 | 34.3 | 0.87 |
| AD S64 | Dolomitised sabkha ramp sands & mud | 68.66 | 0.737 | 0.36 | 0.31 | L2 | 34.8 | 0.96 |
| 905/14 | Carbonate slope sediment | 66.31 | 0.923 | 0.39 | 1.98 | L3 | 34.5 | 0.82 |
| AD S25 | Dolomitised sabkha ramp sands & mud | 64.51 | 0.117 | 0.75 | BD | L2 | 37.4 | 0.95 |
| AD B8 | Dolomitised sabkha ramp sands & mud | 60.54 | 0.132 | 0.52 | BD | L1 | 35.1 | 1.04 |
| Strom unlith | Microbial carbonate & organic matter | 59.33 | 0.231 | 0.94 | 2.12 | L3 | 27.4 | 1.28 |
| AD S31 | Dolomitised sabkha ramp sands & mud | 54.86 | 0.089 | 0.54 | BD | L1 | 30.6 | 1.04 |
| AD S67 | Dolomitised sabkha ramp sands & mud | 52.02 | 0.415 | 0.44 | 0.65 | L2 | 28.4 | 0.93 |
| Abad Marl | Pelagic diatom/carbonate | 41.53 | 2.086 | 0.37 | 0.31 | L1 | 55.1 | 1.09 |
| AD S70 | Dolomitised sabkha ramp sands & mud | 33.45 | 0.383 | 0.43 | 0.19 | L1 | 36.6 | 0.94 |
| AD S21 | Dolomitised sabkha ramp sands & mud | 32.24 | 0.644 | 0.39 | 0.09 | L1 | 29.4 | 0.91 |
| AD S36 | Dolomitised sabkha ramp sands & mud | 30.37 | 0.408 | 0.65 | 0.44 | A | 26.9 | 0.86 |

that is 50% CaCO$_3$ will attack 40% of the total carbonate, which for dolomitic rocks will result in contributions from contaminant phases (Fig. 2). This highlights the additional care that must be taken when dealing with impure or dolomitised samples, and we suggest using %CaCO$_3$ to recalculate the amount of acid required for each leach based on the actual carbonate content, in contrast to methods used here. Unlithified sediments may require different treatment to carbonate rocks as phases such as (oxyhydr)oxide and organic coatings would be more labile in sediments, and additional steps to remove them prior to carbonate dissolution may be necessary.

We recommend that REY studies are, in general, confined to pure carbonates with >85% CaCO$_3$. Prior measurement of %CaCO$_3$ can help to exclude samples that are unlikely to be successfully leached for REY. However, %CaCO$_3$ < 85% should not be used to screen REY data, as data quality should be assessed predominantly using Y/Ho > 36, BSI, $\sum$REE, Yb/Nd and cross-plots with major element and isotopic indicators of diagenesis or contaminants. The optimal leaching procedure for carbonates is highly dependent on the purity and extent of dolomitisation.

### 4.3. Application to palaeo-redox

Negative Ce anomalies preserved in carbonate sediments and rocks are a robust indication that a sample precipitated in an oxic environment, but the absence of any Ce anomaly is somewhat equivocal. The sample may have formed in an anoxic water column, or may have formed in oxic waters with no Ce anomaly, or the anomaly may have been obscured due to contamination during leaching. Further, some carbonate phases may fractionate REY during precipitation, and not record appropriate Ce anomalies that reflect the overlying water column. Ce anomaly transfer to the sediment record probably also relates to sedimentation rate and hard ground formation (Elderfield and Greaves, 1982). Different carbonates record different REY patterns, and therefore REY can only be reliably interpreted if the genesis of a carbonate rock or sediment is reasonably well-understood.

Although negative Ce anomalies are ubiquitous in most modern oxygenated waters, a negative Ce anomaly may be absent in near-shore or
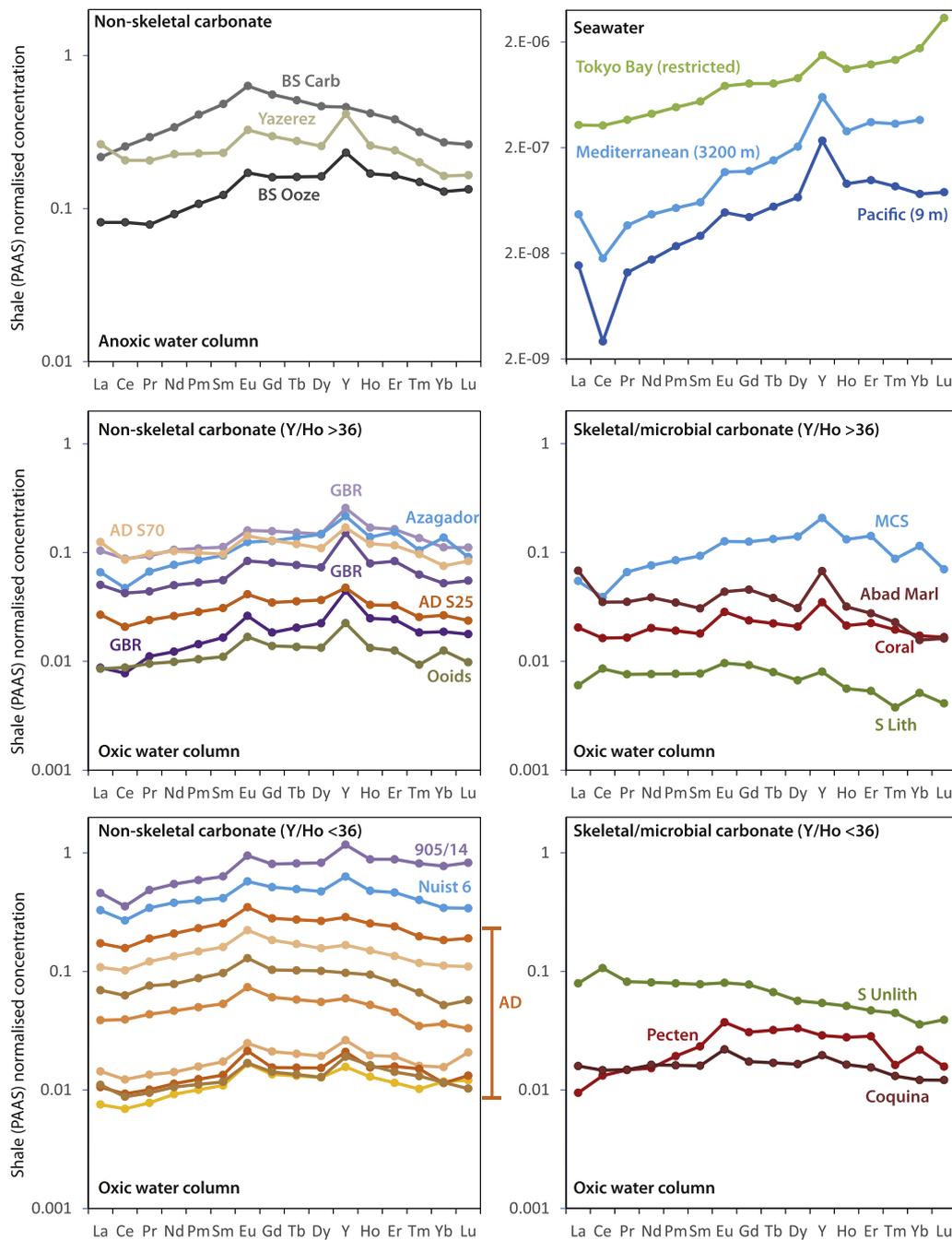
**Fig. 9.** REY patterns for modern skeletal/microbial and nonskeletal carbonate samples from both oxic and anoxic settings (Clarkson et al., 2014). The optimal REY pattern has been selected from a range of different leaching techniques (see Table 2). Modern REY data in top right panel are from the Pacific Ocean, De Baar et al. (1985a); the Mediterranean Sea, Bau et al. (1997) and restricted coastal waters in Tokyo Bay, Nozaki and Zhang (1995). Theoretical Pm values are calculated as $(Nd_{SN} + Sm_{SN})/2$.

restricted settings. For deeper water samples with high siliciclastic components (<85% CaCO$_3$), Ce anomalies may be present within the authigenic carbonate phase, but are commonly obscured by REY from partial leaching of clays, which have high REY concentrations. This may mean that some existing REY studies may contain contributions from non-carbonate phases, which is likely to result in the loss of any potential Ce anomaly, and a false indication of anoxia.

Fe-speciation and Ce anomalies both record water column redox conditions, but they respond over regional and local scales, respectively, and at different oxygen fugacities. Fe-speciation can distinguish oxic from anoxic ferruginous or euxinic conditions, but it cannot distinguish partially oxygenated from fully oxygenated conditions. Cerium anomalies may be more responsive to low oxygen levels, as negative anomalies develop to their full strength where particulate Mn (oxyhydr)oxides are

at a maximum concentration, and then are eroded throughout manganous or ferruginous waters (German et al., 1991), sometimes producing a distinctive positive anomaly (Bau et al., 1997; de Baar et al., 1988; De Carlo and Green, 2002; Planavsky et al., 2010; Slack et al., 2007). Here, we present Fe-speciation and Ce anomaly data together for the Nama Group and modern samples (Clarkson et al., 2014; Wood et al., 2015).

Initial calibration of Fe-speciation in carbonate rich lithologies suggests that samples with sufficient Fe (>0.5 wt%) record accurate Fe$_{HR}$/Fe$_T$ ratios, but further work is required to understand the distribution of Fe in carbonates under different early diagenetic and lithification scenarios (Clarkson et al., 2014). Due to the tendency for oxic carbonates to have low Fe$_T$ (<0.5 wt%), they are more subject to non-depositional enrichments in Fe$_{HR}$ that result in spurious Fe$_{HR}$/Fe$_T$ ratios. Although low Fe$_T$ (<0.5 wt%) may be consistent with oxic conditions, Fe$_T$ > 0.5 wt%
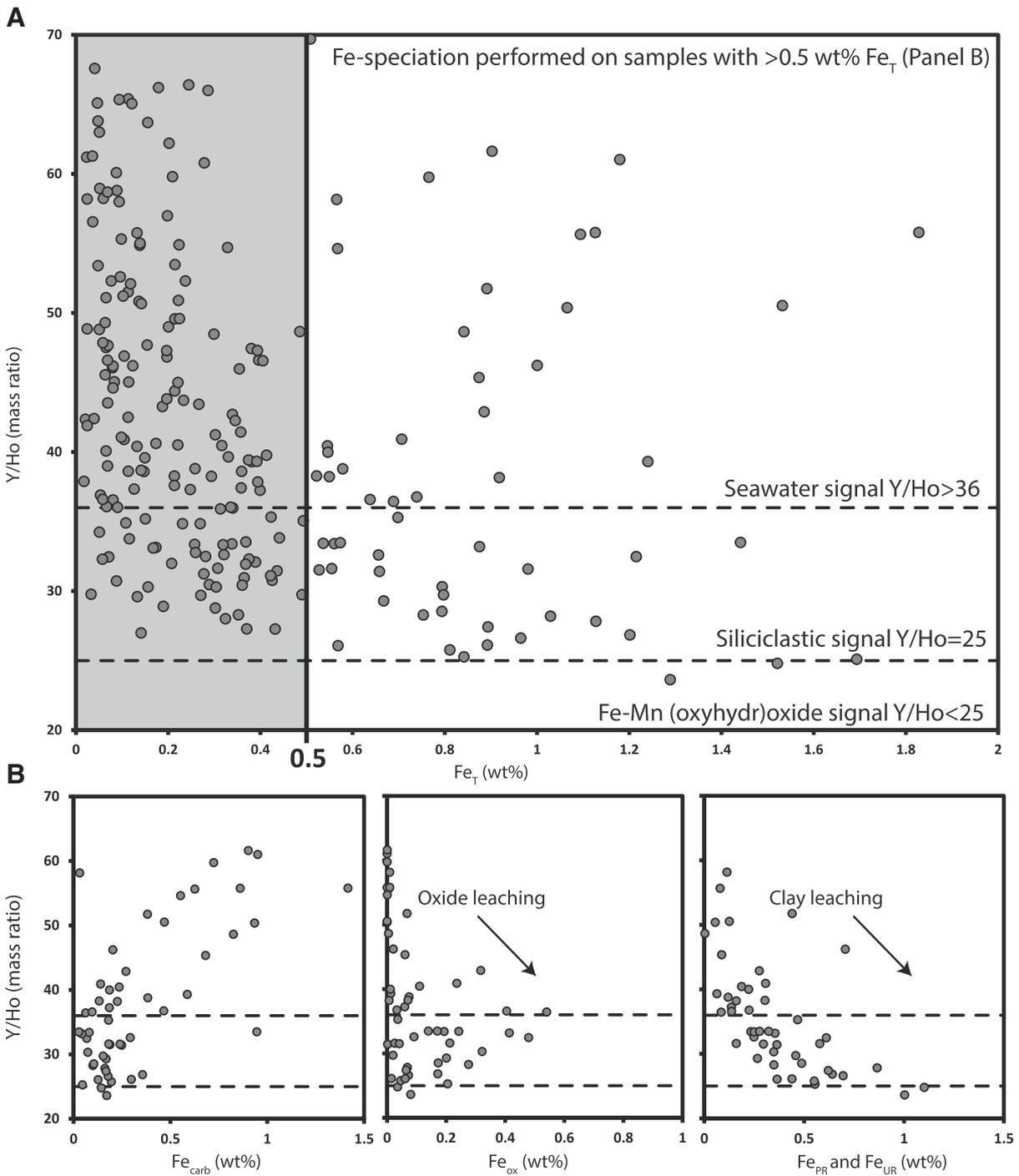
**Fig. 10.** Y anomalies for Zwartmodder, Zebra River, Omkyk and Brak are plotted against $Fe_T$ (A). Samples with positive Y anomalies, in general, have low FeT. For samples with >0.5 wt% $Fe_T$, a breakdown of the different Fe phases is also shown (B). Y anomalies are unaffected by high carbonate Fe contents, but are reduced in samples with higher Fe oxide or clay contents (approximated as $Fe_{UR}$ and $Fe_{PR}$). Dashed lines indicate key threshold values: 25 is the Y/Ho ratio for shale, and >36 is a commonly used threshold value for carbonate REY signals originating from seawater. Fe-Mn (oxyhydr)oxides may have negative Y anomalies compared with shale (<25). The y-axis has a consistent scale across the row in panel B. Fe-speciation data from Wood et al. (2015).

and $Fe_{HR}/Fe_T < 0.22$ is needed for a robust interpretation of oxic conditions. Under anoxic conditions $Fe_T$ enrichments can be seen in carbonates, present as $Fe_{HR}$. This is far greater than can be accounted for under normal oxic deposition, where trace amounts (0.1 wt%) of Fe may be incorporated into carbonates, or precipitate as Fe-Mn coatings. Thus high $Fe_T$ (>0.5 wt%) and high $Fe_{HR}/Fe_T$ (>0.38) values for carbonates can be used to identify anoxic conditions, where late stage dolomitization and diagenetic Fe-enrichments can be discounted. Therefore, Fe-speciation is more useful for identifying anoxic carbonates, which tend towards higher $Fe_T$, than oxic carbonates.

Anoxic carbonates would not show a negative Ce anomaly. However, the absence of a Ce anomaly in carbonates appears to be inconclusive for identifying redox conditions, as the anomaly may not always be present in oxic waters, and it may not be faithfully recorded in some carbonate sediments. Further, impure samples (<85% CaCO₃) may not be suitable for leaching, as the carbonate-bound seawater REY signal is obscured by even small amounts of clay leaching. Pure samples (>85% CaCO₃) often have lower detrital contents and hence insufficient $Fe_T$ for effective Fe-speciation analysis, as a high proportion of siliciclastic/detrital bound Fe helps to buffer the impact of additional $Fe_{HR}$ inputs.
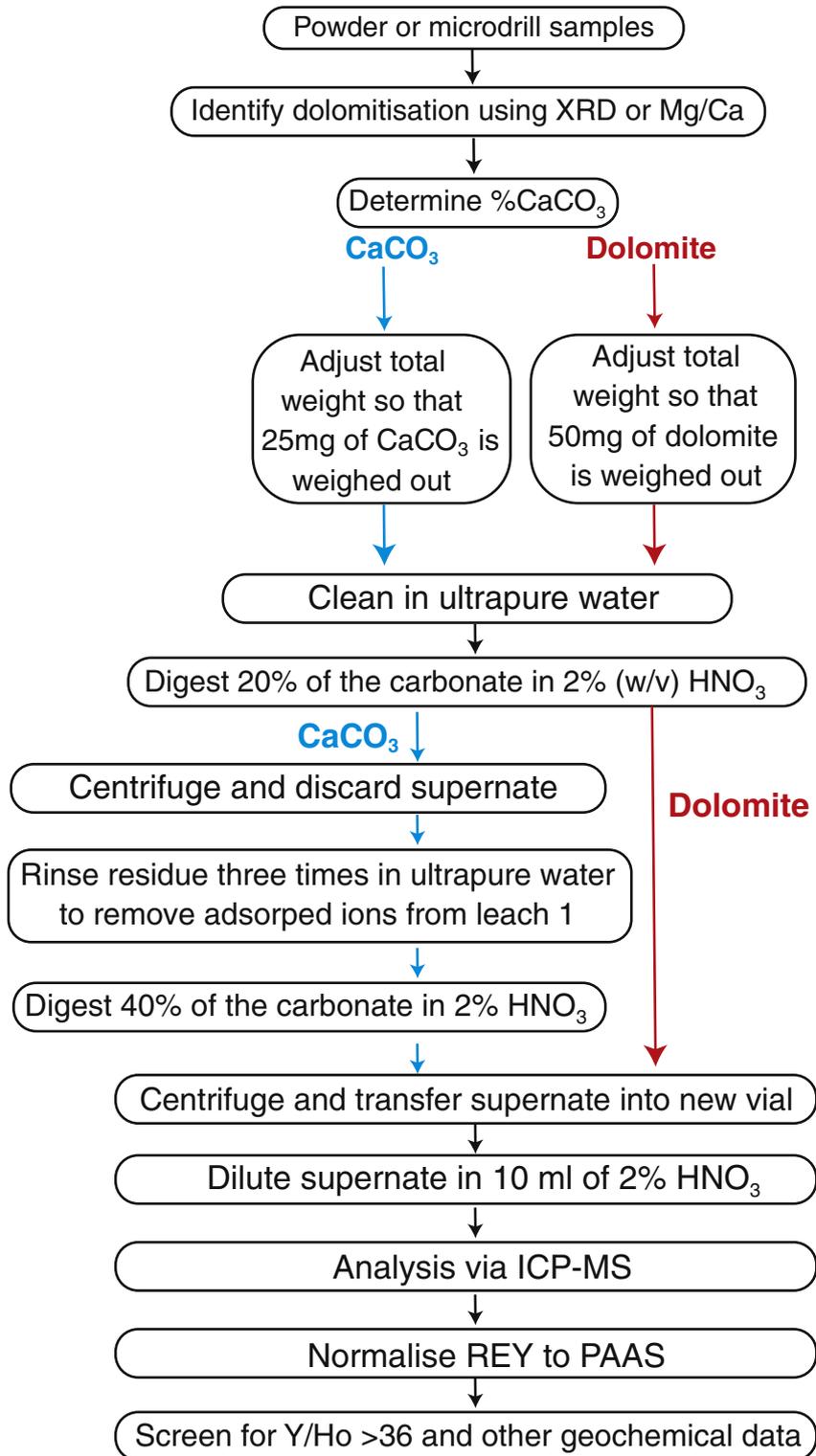
```
┌─────────────────────────────────────┐
│     Powder or microdrill samples     │
└─────────────────────────────────────┘
                 ↓
┌─────────────────────────────────────┐
│  Identify dolomitisation using XRD   │
│              or Mg/Ca                 │
└─────────────────────────────────────┘
                 ↓
┌─────────────────────────────────────┐
│        Determine %CaCO₃              │
└─────────────────────────────────────┘
```

CaCO₃       Dolomite

Figure 11 flowchart:

- **Determine %CaCO$_3$**
  - CaCO$_3$ path: Adjust total weight so that 25mg of CaCO$_3$ is weighed out
  - Dolomite path: Adjust total weight so that 50mg of dolomite is weighed out
- Clean in ultrapure water
- Digest 20% of the carbonate in 2% (w/v) HNO$_3$
  - **CaCO$_3$** path:
    - Centrifuge and discard supernate
    - Rinse residue three times in ultrapure water to remove adsorbed ions from leach 1
    - Digest 40% of the carbonate in 2% HNO$_3$
  - **Dolomite** path continues directly:
- Centrifuge and transfer supernate into new vial
- Dilute supernate in 10 ml of 2% HNO$_3$
- Analysis via ICP-MS
- Normalise REY to PAAS
- Screen for Y/Ho >36 and other geochemical data

**Fig. 11.** A recommended method for selective carbonate digestion in calcites (blue) and dolomites (red), based on samples used in this study. This is a guide only, and the optimal leaching procedure will vary depending on purity and dolomitisation, and should be assessed on a case-by-case basis.

Of the modern samples plotted in Fig. 12, only one meets the criteria to produce effective results using both techniques. Therefore, we recommend the use of Fe-speciation to identify anoxia in carbonates, while Ce anomalies are better for identifying oxic conditions in the presence of low Fe$_T$, providing a powerful combination of techniques for the independent identification of redox conditions in mixed carbonate sections with varying siliciclastic components.

## 5. Conclusions

Variability in REY patterns as a result of the leaching procedure can be as large as the natural variability in REY patterns in seawater. Comparison of REY patterns with Fe-speciation data shows that leaching of clays and Fe oxides can reduce Y anomalies and obscure potential Ce anomalies. To obtain seawater REY patterns and minimise contributions from non-
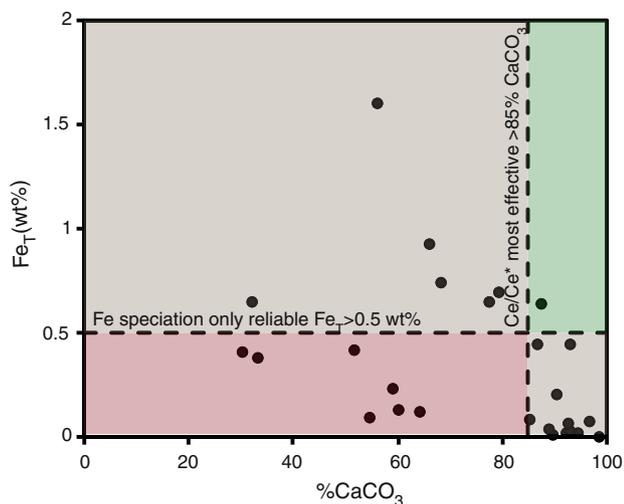
**Fig. 12.** Cross plot of total wt% Fe (Fe$_T$) against purity (%CaCO$_3$) for the modern carbonate samples used in this study. Fe-speciation is an effective redox proxy when Fe$_T$ is above 0.5 wt%. Seawater REY patterns are more likely to be extracted successfully from the carbonate phase for samples with >85% CaCO$_3$. In the red zone neither proxy is optimised, and in the green both are optimised, but very few samples will fall into this zone. In the brown zone, only one proxy is likely to be effective.

carbonate phases we recommend a partial leaching procedure. The optimal leach will vary depending on the purity of the sample, but for calcites with >85%CaCO$_3$, we have demonstrated best results from application of a pre-leach of ~20% of the sample, followed by a partial leach of ~40% of the sample. This can be done effectively using 2% nitric acid. Care must be taken to identify dolomitised samples as they respond differently to leaching. This leaching method may be widely applicable to trace metal work in carbonate rocks. Ce anomalies are sometimes absent in oxic samples, but if present provide a robust indication that the sample formed in an oxic environment. Not all forms of carbonate, particularly skeletal carbonates, accurately record seawater REY. Ce anomalies are most effective at identifying oxic conditions in samples with low siliciclastic components, whereas Fe-speciation is most effective at identifying anoxic conditions in samples with high Fe contents (often from deeper water settings with higher siliciclastic components). The combination of Fe-speciation with Ce anomalies can provide a powerful redox tool in carbonate settings.

## Acknowledgements

## Appendix A. Supplementary data

Supplementary data to this article can be found online at http://dx.doi.org/10.1016/j.chemgeo.2016.06.027.

## References

Abanda, P.A., Hannigan, R.E., 2006. Effect of diagenesis on trace element partitioning in shales. Chem. Geol. 230, 42–59. http://dx.doi.org/10.1016/j.chemgeo.2005.11.011.

Analytical Methods Committee, 1960. Methods for the destruction of organic matter. Analyst 85, 643–656.

Bailey, T., McArthur, J., Prince, H., Thirlwall, M., 2000. Dissolution methods for strontium isotope stratigraphy: whole rock analysis. Chem. Geol. 167, 313–319.

Banner, J.L., Hanson, G.N., Meyers, W.J., 1988. Rare earth element and Nd isotopic variations in regionally extensive dolomites from the Burlington-Keokuk Formation (Mississippian): implications for REE mobility during carbonate diagenesis. J. Sediment. Res. 58.

Bau, M., 1999. Scavenging of dissolved yttrium and rare earths by precipitating iron oxyhydroxide: experimental evidence for Ce oxidation, Y-Ho fractionation, and lanthanide tetrad effect. Geochim. Cosmochim. Acta 63, 67–77.

Bau, M., Dulski, P., 1996. Distribution of yttrium and rare-earth elements in the Penge and Kuruman iron-formations, Transvaal Supergroup, South Africa. Precambrian Res. 79, 37–55.

Bau, M., Möller, P., Dulski, P., 1997. Yttrium and lanthanides in eastern Mediterranean seawater and their fractionation during redox-cycling. Mar. Chem. 56, 123–131. http://dx.doi.org/10.1016/S0304-4203(96)00091-6.

Bau, M., Schmidt, K., Koschinsky, A., Hein, J., Kuhn, T., Usui, A., 2014. Discriminating between different genetic types of marine ferro-manganese crusts and nodules based on rare earth elements and yttrium. Chem. Geol. 381, 1–9.

Bodin, S., Godet, A., Westermann, S., Föllmi, K.B., 2013. Secular change in northwestern Tethyan water-mass oxygenation during the late Hauterivian–early Aptian. Earth Planet. Sci. Lett. 374, 121–131. http://dx.doi.org/10.1016/j.epsl.2013.05.030.

Bolhar, R., Kamber, B.S., Moorbath, S., Fedo, C.M., Whitehouse, M.J., 2004. Characterisation of early Archaean chemical sediments by trace element signatures. Earth Planet. Sci. Lett. 222, 43–60. http://dx.doi.org/10.1016/j.epsl.2004.02.016.

Bolhar, R., Van Kranendonk, M.J., 2007. A non-marine depositional setting for the northern Fortescue Group, Pilbara Craton, inferred from trace element geochemistry of stromatolitic carbonates. Precambrian Res. 155, 229–250. http://dx.doi.org/10.1016/j.precamres.2007.02.002.

Byrne, R.H., Kim, K.-H., 1990. Rare earth element scavenging in seawater. Geochim. Cosmochim. Acta 54, 2645–2656. http://dx.doi.org/10.1016/0016-7037(90)90002-3.

Byrne, R.H., Liu, X., Schijf, J., 1996. The influence of phosphate coprecipitation on rare earth distributions in natural waters. Geochim. Cosmochim. Acta 60, 3341–3346. http://dx.doi.org/10.1016/0016-7037(96)00197-4.

Carmichael, S.K., Ferry, J.M., 2008. Formation of replacement dolomite in the Latemar carbonate buildup, Dolomites, northern Italy: Part 2. Origin of the dolomitizing fluid and the amount and duration of fluid flow. Am. J. Sci. 308, 885–904. http://dx.doi.org/10.2475/08.2008.01.

Castanier, S., 1999. Ca-carbonates precipitation and limestone genesis — the microbiogeologist point of view. Sediment. Geol. 126, 9–23. http://dx.doi.org/10.1016/S0037-0738(99)00028-7.

Chen, J., Algeo, T.J., Zhao, L., Chen, Z.-Q., Cao, L., Zhang, L., Li, Y., 2015. Diagenetic uptake of rare earth elements by bioapatite, with an example from Lower Triassic conodonts of South China. Earth-Sci. Rev. 149, 181–202.

Chou, L., Garrels, R.M., Wollast, R., 1989. Comparative study of the kinetics and mechanisms of dissolution of carbonate minerals. Chem. Geol. Kinet. Geochem. 78, 269–282. http://dx.doi.org/10.1016/0009-2541(89)90063-6.

Clarkson, M.O., Poulton, S.W., Guilbaud, R., Wood, R.A., 2014. Assessing the utility of Fe/Al and Fe-speciation to record water column redox conditions in carbonate-rich sediments. Chem. Geol. 382, 111–122.

De Baar, H.J., Brewer, P.G., Bacon, M.P., 1985b. Anomalies in rare earth distributions in seawater: Gd and Tb. Geochim. Cosmochim. Acta 49, 1961–1969.

De Baar, H.J., German, C.R., Elderfield, H., van Gaans, P., 1988. Rare earth element distributions in anoxic waters of the Cariaco Trench. Geochim. Cosmochim. Acta 52, 1203–1219. http://dx.doi.org/10.1016/0016-7037(88)90275-X.

De Baar, H.J.W., 1991. On cerium anomalies in the Sargasso Sea. Geochim. Cosmochim. Acta 55, 2981–2983. http://dx.doi.org/10.1016/0016-7037(91)90463-F.

De Baar, H.J.W., Bacon, M.P., Brewer, P.G., Bruland, K.W., 1985a. Rare earth elements in the Pacific and Atlantic Oceans. Geochim. Cosmochim. Acta 49, 1943–1959. http://dx.doi.org/10.1016/0016-7037(85)90089-4.

De Carlo, E.H., Green, W.J., 2002. Rare earth elements in the water column of Lake Vanda, McMurdo Dry Valleys, Antarctica. Geochim. Cosmochim. Acta 66, 1323–1333. http://dx.doi.org/10.1016/S0016-7037(01)00861-4.

De Carlo, E.R., 2000. Rare earth element fractionation in hydrogenetic Fe-Mn crusts: the influence of carbonate complexation and phosphatization on Sm/Yb ratios. Soc. Sediment. Geol. 66, 271–285.

Douville, E., Bienvenu, P., Charlou, J.L., Donval, J.P., Fouquet, Y., Appriou, P., Gamo, T., 1999. Yttrium and rare earth elements in fluids from various deep-sea hydrothermal systems. Geochim. Cosmochim. Acta 63, 627–643. http://dx.doi.org/10.1016/S0016-7037(99)00024-1.

Edmonds, H.N., German, C.R., 2004. Particle geochemistry in the Rainbow hydrothermal plume, Mid-Atlantic Ridge. Geochim. Cosmochim. Acta 68, 759–772.

Elderfield, H., Greaves, M.J., 1982. The rare earth elements in seawater. Nature 296, 214–219. http://dx.doi.org/10.1038/296214a0.

Elderfield, H., Upstill-Goddard, R., Sholkovitz, E.R., 1990. The rare earth elements in rivers, estuaries, and coastal seas and their significance to the composition of ocean waters. Geochim. Cosmochim. Acta 54, 971–991. http://dx.doi.org/10.1016/0016-7037(90)90432-K.

Freslon, N., Bayon, G., Toucanne, S., Bermell, S., Bollinger, C., Chéron, S., Etoubleau, J., Germain, Y., Khripounoff, A., Ponzevera, E., Rouget, M.-L., 2014. Rare earth elements and neodymium isotopes in sedimentary organic matter. Geochim. Cosmochim. Acta 140, 177–198. http://dx.doi.org/10.1016/j.gca.2014.05.016.

Frimmel, H.E., 2010. On the reliability of stable carbon isotopes for Neoproterozoic chemostratigraphic correlation. Precambrian Res. 182, 239–253. http://dx.doi.org/10.1016/j.precamres.2010.01.003.

German, C.R., Elderfield, H., 1990. Application of the Ce anomaly as a paleoredox indicator: the ground rules. Paleoceanography 5, 823. http://dx.doi.org/10.1029/PA005i005p00823.

German, C.R., Holliday, B.P., Elderfield, H., 1991. Redox cycling of rare earth elements in the suboxic zone of the Black Sea. Geochim. Cosmochim. Acta 55, 3553–3558. http://dx.doi.org/10.1016/0016-7037(91)90055-A.

Haley, B.A., Klinkhammer, G.P., McManus, J., 2004. Rare earth elements in pore waters of marine sediments. Geochim. Cosmochim. Acta 68, 1265–1279. http://dx.doi.org/10.1016/j.gca.2003.09.012.

Hill, I.G., Worden, R.H., Meighan, I.G., 2000. Yttrium: the immobility-mobility transition during basaltic weathering. Geology 28, 923–926.

Himmler, T., Bach, W., Bohrmann, G., Peckmann, J., 2010. Rare earth elements in authigenic methane-seep carbonates as tracers for fluid composition during early diagenesis. Chem. Geol. 277, 126–136. http://dx.doi.org/10.1016/j.chemgeo.2010.07.015.

Himmler, T., Haley, B.A., Torres, M.E., Klinkhammer, G.P., Bohrmann, G., Peckmann, J., 2013. Rare earth element geochemistry in cold-seep pore waters of Hydrate Ridge, northeast Pacific Ocean. Geo-Mar. Lett. 33, 369–379. doi:10.1007/s00367-013-0334-2.

Hu, Y., Feng, D., Peckmann, J., Roberts, H.H., Chen, D., 2014. New insights into cerium anomalies and mechanisms of trace metal enrichment in authigenic carbonate from hydrocarbon seeps. Chem. Geol. 381, 55–66.

James, R., Elderfield, H., Palmer, M., 1995. The chemistry of hydrothermal fluids from the Broken Spur site, 29°N Mid-Atlantic Ridge. Geochim. Cosmochim. Acta 59, 651–659.

Jarvis, K.E., Gray, A.L., McCurdy, E., 1989. Avoidance of spectral interference on europium in inductively coupled plasma mass spectrometry by sensitive measurement of the doubly charged ion. J. Anal. At. Spectrom. 4, 743–747.

Johannesson, K.H., Hawkins Jr., D.L., Cortés, A., 2006. Do Archean chemical sediments record ancient seawater rare earth element patterns? Geochim. Cosmochim. Acta 70, 871–890. http://dx.doi.org/10.1016/j.gca.2005.10.013.

Johannesson, K.H., Telfeyan, K., Chevis, D.A., Rosenheim, B.E., Leybourne, M.I., 2014. Rare earth elements in stromatolites — 1. Evidence that Modern terrestrial stromatolites fractionate rare earth elements during incorporation from ambient waters. Evolution of Archean Crust and Early Life. Springer, pp. 385–411.

Kahle, C.F., 1965. Possible roles of clay minerals in the formation of dolomite. J. Sediment. Res. 35, 448–453.

Kakuwa, Y., Matsumoto, R., 2006. Cerium negative anomaly just before the Permian and Triassic boundary event – the upward expansion of anoxia in the water column. Palaeogeogr. Palaeoclimatol. Palaeoecol. 229, 335–344.

Knauss, K.G., Wolery, T.J., 1989. Muscovite dissolution kinetics as a function of pH and time at 70 °C. Geochim. Cosmochim. Acta 53, 1493–1501. http://dx.doi.org/10.1016/0016-7037(89)90232-9.

Kraemer, D., Kopf, S., Bau, M., 2015. Oxidative mobilization of cerium and uranium and enhanced release of "immobile" high field strength elements from igneous rocks in the presence of the biogenic siderophore desferrioxamine B. Geochim. Cosmochim. Acta 165, 263–279. http://dx.doi.org/10.1016/j.gca.2015.05.046.

Lawrence, M.G., Greig, A., Collerson, K.D., Kamber, B.S., 2006. Rare Earth Element and Yttrium Variability in South East Queensland Waterways. Aquat. Geochem. 12, 39–72. http://dx.doi.org/10.1007/s10498-005-4471-8.

Li, D., Shields-Zhou, G.A., Ling, H.-F., Thirlwall, M., 2011. Dissolution methods for strontium isotope stratigraphy: guidelines for the use of bulk carbonate and phosphorite rocks. Chem. Geol. 290, 133–144. http://dx.doi.org/10.1016/j.chemgeo.2011.09.004.

Ling, H.-F., Chen, X., Li, D., Wang, D., Shields-Zhou, G.A., Zhu, M., 2011. Cerium anomaly variations in Ediacaran–earliest Cambrian carbonates from the Yangtze Gorges area, South China: implications for oxygenation of coeval shallow seawater. Precambrian Res. http://dx.doi.org/10.1016/j.precamres.2011.10.011.

Liu, X., Byrne, R.H., 1997. Rare earth and yttrium phosphate solubilities in aqueous solution. Geochim. Cosmochim. Acta 61, 1625–1633. http://dx.doi.org/10.1016/S0016-7037(97)00037-9.

Liu, Y.-G., Miah, M., Schmitt, R., 1988. Cerium: a chemical tracer for paleo-oceanic redox conditions. Geochim. Cosmochim. Acta 52, 1361–1371.

Lokier, S., Steuber, T., 2008. Quantification of carbonate-ramp sedimentation and progradation rates for the Late Holocene Abu Dhabi shoreline. J. Sediment. Res. 78, 423–431. http://dx.doi.org/10.2110/jsr.2008.049.

Lu, Z., Jenkyns, H.C., Rickaby, R.E.M., 2010. Iodine to calcium ratios in marine carbonate as a paleo-redox proxy during oceanic anoxic events. Geology 38, 1107–1110. http://dx.doi.org/10.1130/G31145.1.

Martin, E.E., Blair, S.W., Kamenov, G.D., Scher, H.D., Bourbon, E., Basak, C., Newkirk, D.N., 2010. Extraction of Nd isotopes from bulk deep sea sediments for paleoceanographic studies on Cenozoic time scales. Chem. Geol. 269, 414–431. http://dx.doi.org/10.1016/j.chemgeo.2009.10.016.

Mazumdar, A., Tanaka, K., Takahashi, T., Kawabe, I., 2003. Characteristics of rare earth element abundances in shallow marine continental platform carbonates of Late Neoproterozoic successions from India. Geochem. J. 37, 277–289. http://dx.doi.org/10.2343/geochemj.37.277.

McArthur, J., Walsh, J., 1984. Rare-earth geochemistry of phosphorites. Chem. Geol. 47, 191–220.

Meyer, E.E., Quicksall, A.N., Landis, J.D., Link, P.K., Bostick, B.C., 2012. Trace and rare earth elemental investigation of a Sturtian cap carbonate, Pocatello, Idaho: evidence for ocean redox conditions before and during carbonate deposition. Precambrian Res. 192–195, 89–106. http://dx.doi.org/10.1016/j.precamres.2011.09.015.

Möller, P., Bau, M., 1993. Rare-earth patterns with positive cerium anomaly in alkaline waters from Lake Van, Turkey. Earth Planet. Sci. Lett. 117, 671–676. http://dx.doi.org/10.1016/0012-821X(93)90110-U.

Nothdurft, L.D., Webb, G.E., Kamber, B.S., 2004. Rare earth element geochemistry of Late Devonian reefal carbonates, Canning Basin, Western Australia: confirmation of a seawater REE proxy in ancient limestones. Geochim. Cosmochim. Acta 68, 263–283. http://dx.doi.org/10.1016/S0016-7037(03)00422-8.

Nozaki, Y., Zhang, J., 1995. The rare earth elements and yttrium in the coastal/offshore mixing zone of Tokyo Bay waters and the Kuroshio. Biogeochem. Process. Ocean Flux West. Pac. 171–184.

Ohta, A., Kawabe, I., 2001. REE (III) adsorption onto Mn dioxide ($MnO_2$) and Fe oxyhydroxide: Ce(III) oxidation by $MnO_2$. Geochim. Cosmochim. Acta 65, 695–703.

Planavsky, N., Bekker, A., Rouxel, O.J., Kamber, B., Hofmann, A., Knudsen, A., Lyons, T.W., 2010. Rare earth element and yttrium compositions of Archean and Paleoproterozoic Fe formations revisited: new perspectives on the significance and mechanisms of deposition. Geochim. Cosmochim. Acta 74, 6387–6405. http://dx.doi.org/10.1016/j.gca.2010.07.021.

Poulton, S.W., Canfield, D.E., 2005. Development of a sequential extraction procedure for iron: implications for iron partitioning in continentally derived particulates. Chem. Geol. 214, 209–221.

Pourmand, A., Dauphas, N., Ireland, T.J., 2012. A novel extraction chromatography and MC-ICP-MS technique for rapid analysis of REE, Sc and Y: Revising CI-chondrite and Post-Archean Australian Shale (PAAS) abundances. Chem. Geol. 291, 38–54. http://dx.doi.org/10.1016/j.chemgeo.2011.08.011.

Pourret, O., Davranche, M., Gruau, G., Dia, A., 2008. New insights into cerium anomalies in organic-rich alkaline waters. Chem. Geol. 251, 120–127. http://dx.doi.org/10.1016/j.chemgeo.2008.03.002.

Riding, R., Fralick, P., Liang, L., 2014. Identification of an Archean marine oxygen oasis. Precambrian Res. 251, 232–237.

Schroder, S., Grotzinger, J.P., 2007. Evidence for anoxia at the Ediacaran-Cambrian boundary: the record of redox sensitive trace elements and rare earth elements in Oman. J. Geol. Soc. 164, 175–187.

Shields, G., Stille, P., Brasier, M.D., Atudorei, N.-V., 1997. Stratified oceans and oxygenation of the late Precambrian environment: a post glacial geochemical record from the Neoproterozoic of W. Mongolia. Terra Nova 9, 218–222. http://dx.doi.org/10.1111/j.1365-3121.1997.tb00016.x.

Shields, G., Webb, G., 2004. Has the REE Composition of Seawater Changed Over Geological Time? 204 pp. 103–107

Sholkovitz, E.R., 1989. Artifacts associated with the chemical leaching of sediments for rare-earth elements. Chem. Geol. 77, 47–51. http://dx.doi.org/10.1016/0009-2541(89)90014-4.

Sholkovitz, E.R., Landing, W.M., Lewis, B.L., 1994. Ocean particle chemistry: The fractionation of rare earth elements between suspended particles and seawater. Geochim. Cosmochim. Acta 58, 1567–1579. http://dx.doi.org/10.1016/0016-7037(94)90559-2.

Sholkovitz, E., Shen, G.T., 1995. The incorporation of rare earth elements in modern coral. Geochim. Cosmochim. Acta 59, 2749–2756. http://dx.doi.org/10.1016/0016-7037(95)00170-5.

Slack, J., Grenne, T., Bekker, A., Rouxel, O., Lindberg, P., 2007. Suboxic deep seawater in the late Paleoproterozoic: evidence from hematitic chert and iron formation related to seafloor-hydrothermal sulfide deposits, central Arizona, USA. Earth Planet. Sci. Lett. 255, 243–256.

Soyol-Erdene, T.-O., Huh, Y., 2013. Rare earth element cycling in the pore waters of the Bering Sea Slope (IODP Exp. 323). Chem. Geol. 358, 75–89. http://dx.doi.org/10.1016/j.chemgeo.2013.08.047.

Sunda, W.G., Huntsman, S.A., 1988. Effect of sunlight on redox cycles of manganese in the southwestern Sargasso Sea. Deep-Sea Res. I Oceanogr. Res. Pap. 35, 1297–1317.

Taylor, S.R., McLennan, S.M., Armstrong, R.L., Tarney, J., 1981. The composition and evolution of the continental crust: rare earth element evidence from sedimentary rocks [and discussion]. Philos. Trans. R. Soc. Lond. Ser. Math. Phys. Sci. 301, 381–399. http://dx.doi.org/10.1098/rsta.1981.0119.

Tessier, A., Campbell, P.G.C., Bisson, M., 1979. Sequential extraction procedure for the speciation of particulate trace metals. Anal. Chem. 51, 844–851. http://dx.doi.org/10.1021/ac50043a017.

Vasconcelos, C., Warthmann, R., McKenzie, J.A., Visscher, P.T., Bittermann, A.G., van Lith, Y., 2006. Lithifying microbial mats in Lagoa Vermelha, Brazil: Modern Precambrian relics? Sediment. Geol. 185, 175–183. http://dx.doi.org/10.1016/j.sedgeo.2005.12.022.

Webb, G.E., Kamber, B.S., 2000. Rare earth elements in Holocene reefal microbialites: a new shallow seawater proxy. Geochim. Cosmochim. Acta 64, 1557–1565. http://dx.doi.org/10.1016/S0016-7037(99)00400-7.

Webb, G.E., Nothdurft, L.D., Kamber, B.S., Kloprogge, J.T., Zhao, J.-X., 2009. Rare earth element geochemistry of scleractinian coral skeleton during meteoric diagenesis: a sequence through neomorphism of aragonite to calcite. Sedimentology 56, 1433–1463. http://dx.doi.org/10.1111/j.1365-3091.2008.01041.x.

Wood, R., A., 2011. Paleoecology of the earliest skeletal metazoan communities: Implications for early biomineralization. Earth-Sci. Rev. 106, 184–190. http://dx.doi.org/10.1016/j.earscirev.2011.01.011.

Wood, R.A., Poulton, S.W., Prave, A.R., Hoffmann, K.-H., Clarkson, M.O., Guilbaud, R., Lyne, J.W., Tostevin, R., Bowyer, F., Penny, A.M., Curtis, A., Kasemann, S.A., 2015. Dynamic redox conditions control late Ediacaran ecosystems in the Nama Group, Namibia. Precambrian Res. 261, 252–271.

Xiao, S., Shen, B., Tang, Q., Kaufman, A.J., Yuan, X., Li, J., Qian, M., 2014. Biostratigraphic and chemostratigraphic constraints on the age of early Neoproterozoic carbonate successions in North China. Precambrian Res. 246, 208–225. http://dx.doi.org/10.1016/j.precamres.2014.03.004.

Zhang, J., Nozaki, Y., 1998. Behavior of rare earth elements in seawater at the ocean margin: a study along the slopes of the Sagami and Nankai troughs near Japan. Geochim. Cosmochim. Acta 62, 1307–1317. http://dx.doi.org/10.1016/S0016-7037(98)00073-8.

Zhang, K., Zhu, X.-K., Yan, B., 2015. A refined dissolution method for rare earth element studies of bulk carbonate rocks. Chem. Geol. 412, 82–91. http://dx.doi.org/10.1016/j.chemgeo.2015.07.027.

Zhong, S., Mucci, A., 1995. Partitioning of rare earth elements (REEs) between calcite and seawater solutions at 25 °C and 1 atm, and high dissolved REE concentrations. Geochim. Cosmochim. Acta 59, 443–453.

Zhou, Y., Bohor, B.F., Ren, Y., 2000. Trace element geochemistry of altered volcanic ash layers (tonsteins) in Late Permian coal-bearing formations of eastern Yunnan and western Guizhou Provinces, China. Int. J. Coal Geol. 44, 305–324.